Anderson localization of surface plasmons and nonlinear optics of metal-dielectric composites

Andrey K. Sarychev
Department of Physics, New Mexico State University, Las Cruces, New Mexico 88003
and Center for Applied Problems of Electrodynamics, 127412, Moscow, Russia

V. A. Shubin and Vladimir M. Shalaev
Department of Physics, New Mexico State University, Las Cruces, New Mexico 88003
(Received 3 May 1999; revised manuscript received 2 August 1999)

A scaling theory of local-field fluctuations and optical nonlinearities is developed for random metal-dielectric composites near a percolation threshold. The theory predicts that in the optical and infrared spectral ranges the local fields are very inhomogeneous and consist of sharp peaks representing localized surface plasmons. The localization maps the Anderson localization problem described by the random Hamiltonian with both on- and off-diagonal disorder. The local fields exceed the applied field by several orders of magnitudes resulting in giant enhancements of various optical phenomena. The developed theory quantitatively describes enhancement in percolation composites for arbitrary nonlinear optical process. It is shown that enhancement strongly depends on whether a nonlinear multiphoton scattering includes the act of photon subtraction (annihilation). The magnitudes and spectral dependencies of enhancements in optical processes with photon subtraction, such as Raman and hyper-Raman scattering, Kerr refraction, and four-wave mixing, are dramatically different from those in processes without photon subtraction, such as in sum-frequency and high-harmonic generation. At percolation, a dip in dependence of optical processes on the metal concentration is predicted. [S0163-1829(99)15547-4]

I. INTRODUCTION

Local electromagnetic field fluctuations and related enhancement of nonlinear optical phenomena in metal-dielectric composites near percolation threshold (percolation composites) have recently become an area of active studies, because of many fundamental problems involved and the high potential for various applications. Percolation systems are very sensitive to the external electric field since their transport and optical properties are determined by a rather sparse network of conducting channels, and the field concentrates in the "weak" points of the channels. Therefore, composite materials can have much larger nonlinear susceptibilities at zero and finite frequencies than those of its constitutes. The distinguished feature of percolation composites, to amplify nonlinearities of its components, have been recognized very early,[1–6] and nonlinear conductivities and susceptibilities have been intensively studied during the last decade (see, for example, Refs. 7–12).

Here, we consider relatively weak nonlinearities when conductivity $\sigma(E)$ can be expanded in the power series of the applied electric field E, and the leading term, i.e., the linear conductivity $\sigma^{(1)}$, is much larger than others. This situation is typical for various nonlinearities in the optical and infrared spectral ranges considered here. Even weak nonlinearities lead to qualitatively new physical effects. For example, generation of higher harmonics can be much enhanced in percolation composites and bistable behavior of the effective conductivity can occur when the conductivity switches between two stable values, etc.[13] We note that the "languages" of nonlinear currents/conductivities and nonlinear polarizations/susceptibilities (or dielectric constants) are completely equivalent and they will be used here interchangeably.

The local-field fluctuations can be strongly enhanced in the optical and infrared spectral ranges for a composite material containing metal particles that are characterized by the dielectric constant with negative real and small imaginary parts. Then, the enhancement is due to the surface plasmon resonance in metallic granules and their clusters.[7,9,14,15] The strong fluctuations of the local electric field lead to enhancement of various nonlinear effects. Nonlinear percolation composites are potentially of great practical importance[16] as media with intensity-dependent dielectric functions and, in particular, as nonlinear filters and optical bistable elements. The optical response of nonlinear composites can be tuned by controlling the volume fraction and morphology of constitutes.

In our previous paper,[10] we performed numerical simulations for enhancement of various nonlinear optical effects in $2d$ percolation films and developed a scaling approach for high-order moments of the field *magnitudes*, $\langle|E(\mathbf{r})|^n\rangle$. However, nonlinear optical effects depend not only on the magnitude of the field but also on its *phase*, so that a nonlinear signal, in general, is proportional to $\langle|E(\mathbf{r})|^k E^m(\mathbf{r})\rangle$. In this paper, we describe a scaling theory for enhancement of *arbitrary* nonlinear optical process (for both $2d$ and $3d$ percolation composites) and show that enhancement differs significantly for nonlinear optical processes that include photon subtraction (annihilation) and for those that do not. The photon subtraction implies that the corresponding field amplitude in the expression for the nonlinear polarization (current) $P^{(n)}$ is complex conjugated.[17] For example, the optical process known as coherent anti-Stokes Raman scattering is driven by the nonlinear polarization $P^{(3)} \propto E^2(\omega_1)E^*(\omega_2)$,

 ©1999 The American Physical Society

which results in generation of a wave at the frequency $\omega_g = 2\omega_1 - \omega_2$, i.e., in one elementary act of this process, the ω_2 photon is subtracted (annihilated); the corresponding amplitude $E(\omega_2)$ in the expression for $P^{(3)}$ is complex conjugated.

The theory of nonlinear optical processes in metal-dielectric composites is based on the fact that the problem of optical excitations in percolation composites mathematically maps the Anderson transition problem. This allowed us to predict localization of surface plasmons (sp) in percolation composites and describe in detail the localization pattern. We show that the sp eigenstates are localized on the scale much smaller than the wavelength of the incident light. The sp eigenstates with eigenvalues close to zero (resonant modes) are excited most efficiently by the external field. Since the eigenstates are localized and only a small portion of them are excited by the incident beam, the overlapping of the eigenstates can typically be neglected, that significantly simplifies theoretical consideration and allows one to obtain relatively simple expressions for enhancements of linear and nonlinear optical responses. It is important to stress again that the sp-localization length is much smaller than the light wavelength; in that sense, the predicted subwavelength localization of the sp quite differs from the well-known localization of light due to strong scattering in a random homogeneous medium.[18]

We also note that a developed scaling theory of optical nonlinearities in percolation composites opens new means to study the classical Anderson problem, taking advantage of unique characteristics of laser radiation, namely, its coherence and high intensity. For example, our theory predicts that at percolation there is a *minimum* in nonlinear optical responses of metal-dielectric composites, the fact that follows from the Anderson localization of sp modes and can be studied and verified in laser experiments.

In spite of big efforts, most of theoretical considerations of the local optical fields in percolation composites are restricted to mean-field theories and computer simulations (for references, see Refs. 10–12). The effective medium theory[19] that have the virtue of relative mathematical and conceptual simplicity, was extended for the nonlinear response of percolating composites[7,8,20–26] and fractal clusters.[23] For linear problems, predictions of the effective medium theory are usually sensible physically and offer quick insight into problems that are difficult to attack by other means.[7] The effective medium theory, however, has disadvantages typical for all mean-field theories, namely, it diminishes the role of fluctuations in a system. In this approach, it is assumed that local electric fields are the same in the volume occupied by each component of a composite. For example, the effective medium theory predicts that the local electric field should be the same in all metal grains regardless of their local arrangement in a metal-dielectric composite. Therefore the local field is predicted to be almost uniform, in particular, in metal-dielectric composites near percolation. This is, of course, counter-intuitive since percolation represent a phase transition, where according to the basic principles, fluctuations play a crucial role and determine system's physical properties. Moreover, in the optical spectral range, the fluctuations are anticipated to be dramatically enhanced because of the resonance with sp modes of a composite.

In our previous papers we developed rather effective numerical method[27] and performed comprehensive simulations of the local field distribution and various nonlinear effects in two dimensional percolation composites, namely in random metal-dielectric films.[10,28–31] The effective medium approach fails to explain results of the performed computer simulations. It appears that electric fields in such films consist of strongly localized sharp peaks resulting in very inhomogeneous spatial distributions of the local fields. In peaks ("hot" spots), the local fields exceed the applied field by several orders of magnitudes (see, Figs. 1 and 2 here and, e.g., Figs. 2 and 3 in Ref. 10). These peaks are localized in nm-size areas and can be associated with the sp modes of metal clusters in a semicontinuous metal film. The peak distribution is not random but appears to be spatially correlated and organized in some chains. The length of the chains and the average distance between them increase toward the infrared part of the spectrum.

In this paper, we develop the scaling theory of the field spatial distributions and show that there is an important parameter in the scaling theory (missed in our previous consideration), the Anderson localization length ξ_A. We also generalize our previous approach limited to $2d$ systems to include both $2d$ and $3d$ percolation composites. As mentioned, enhancement factors for arbitrary optical nonlinearities are found in the general form.

Note that in the optical range, field distributions in metal fractals have been studied experimentally using near-field scanning optical microscopy allowing a subwavelength resolution.[32,33] The predicted giant local-field fluctuations in the percolation composites have been detected in recent microwave[34] and optic experiments.[35]

The rest of the paper is organized as follows. In Sec. II, we consider local fields and their high-order moment distributions in percolation composites. We also show there that the field distribution maps the Anderson localization problem in quantum mechanics and employ this fact to describe in detail a localization pattern of sp modes. The mapping and scaling arguments are used to obtain the field high-order moments and their dependencies on the frequency of an incident wave and metal concentration, for arbitrary optical nonlinearity. In Sec. III, we calculate enhancement factors for a number of optical processes, namely, Raman and hyper-Raman scattering, Kerr-type nonlinear refraction and absorption, and nth harmonic generation. We show that most of the enhancement originates from strongly localized nanometer-scale areas, where the local electric field has its maxima. Enhancements in these "hot zones" are giant and exceed a "background" nonlinear signal by many orders of magnitude. Concluding discussions are presented in Sec. IV.

II. SCALING THEORY OF FIELD FLUCTUATIONS AND HIGH-ORDER FIELD MOMENTS

In metal-dielectric percolation composites the effective dc conductivity σ_e decreases with decreasing the volume concentration of metal component p and vanishes when the concentration p approaches concentration p_c known as a percolation threshold.[7,15,36] In the vicinity of the percolation threshold p_c, the effective conductivity σ_e is determined by an infinite cluster of percolating (conducting) channels. For

concentration p smaller then the percolation threshold p_c, the effective dc conductivity $\sigma_e=0$, that is the system is a dielectriclike. Therefore, metal-insulator transition takes place at $p=p_c$. Since the metal-insulator transition associated with percolation represents a geometric phase transition one can anticipate that the current and field fluctuations are scale invariant and large.

In percolation composites, however, the fluctuation pattern appears to be quite different from that for a second-order transition, where fluctuations are characterized by the long-range correlation, and their relative magnitudes are of the order of unity, at any point of a system.[37,38] In contrast, for a dc percolation, local electric fields are concentrated at the edges of large metal clusters so that the field maxima (large fluctuations) are separated by distances of an order of the percolation correlation length ξ, which diverges when the metal volume concentration p approaches the percolation threshold p_c.[36,39,40]

We show below that the difference in fluctuations becomes even more striking in the optical spectral range, where the local-field peaks have the resonance nature and, therefore, their relative magnitudes can be up to 10^5, for the linear response, and 10^{20} and more, for nonlinear responses, with distances between the peaks much larger than the percolation correlation length ξ.

In the optical and infrared spectral ranges, the surface plasmon resonances play a crucial role in metal-dielectric composites. To get insight in the high-frequency properties of metals, we first consider a simple model known as a Drude metal that reproduces semiquantitatively the basic optical properties of a metal. In this approach, the dielectric constant of metal grains can be approximated by the Drude formula

$$\epsilon_m(\omega)=\epsilon_b-(\omega_p/\omega)^2/[1+i\omega_\tau/\omega], \tag{1}$$

where ϵ_b is contribution to ϵ_m due to the inter-band transitions, ω_p is the plasma frequency, and $\omega_\tau=1/\tau\ll\omega_p$ is the relaxation rate. In the high-frequency range considered here, losses in metal grains are relatively small, $\omega_\tau\ll\omega$. Therefore, the real part ϵ_m' of the metal dielectric function ϵ_m is much larger (in modulus) than the imaginary part ϵ_m'' ($|\epsilon_m'|/\epsilon_m''\cong\omega/\omega_\tau\gg1$), and ϵ_m' is negative for the frequencies ω less than the renormalized plasma frequency,

$$\tilde{\omega}_p=\omega_p/\sqrt{\epsilon_b}. \tag{2}$$

Thus, the metal conductivity $\sigma_m=-i\omega\epsilon_m/4\pi\cong(\epsilon_b\tilde{\omega}_p/4\pi\omega)[i(1-\omega^2/\tilde{\omega}_p)+\omega_\tau/\omega]$ is characterized by the dominant imaginary part for $\tilde{\omega}_p>\omega\gg\omega_\tau$, i.e., it is of inductive character. Therefore, the metal grains can be modeled as inductances L while the dielectric gaps can be represented by capacitances C. Then, the percolation composite represents a set of randomly distributed L and C elements. The collective surface plasmons excited by the external field, can be thought of as resonances in different $L-C$ circuits, and the excited surface plasmon eigenstates are seen as giant fluctuations of the local field.

A. Local-field distribution in percolation composites with $\epsilon_d=-\epsilon_m'$

We suppose that a percolation composite is illuminated by light and consider local optical field distribution. A typical metal grain size a in the percolation nanocomposites is about few nanometers,[9] that is much smaller than the wavelength λ of the light in the visible and infrared spectral ranges. When wavelength λ is much larger than the particle size a we can introduce potential $\phi(\mathbf{r})$ for the local electric field. Then the local current density $\mathbf{j}$ can be written as $\mathbf{j}(\mathbf{r})=\sigma(\mathbf{r})[-\nabla\phi(\mathbf{r})+\mathbf{E}_0]$, where $\mathbf{E}_0$ is the applied field and $\sigma(\mathbf{r})$ is the local conductivity. In the considered quasistatic case the field distribution problem reduces to solution of the Poisson equation, representing the current conservation law $\mathrm{div}\,\mathbf{j}=0$, namely

$$\nabla\cdot(\sigma(\mathbf{r})[-\nabla\phi(\mathbf{r})+\mathbf{E}_0])=0, \tag{3}$$

where the local conductivity $\sigma(\mathbf{r})$ takes either σ_m or σ_d values, for metal and dielectric components, respectively. It is convenient to rewrite Eq. (3) in terms of the local dielectric constant $\epsilon(\mathbf{r})=4\pi i\sigma(\mathbf{r})/\omega$ as follows

$$\nabla\cdot[\epsilon(\mathbf{r})\nabla\phi(\mathbf{r})]=\mathcal{E}, \tag{4}$$

where $\mathcal{E}=\nabla\cdot[\epsilon(\mathbf{r})\mathbf{E}_0]$. The external field $\mathbf{E}_0$ can be chosen real, while the local potential $\phi(\mathbf{r})$ takes complex values since the metal dielectric constant ϵ_m is complex $\epsilon_m=\epsilon_m'+i\epsilon_m''$ in the optical and infrared spectral ranges. Because of difficulties to find solution to the Poisson Eq. (3) or (4), a great deal of use is made of the tight binding model in which metal and dielectric particles are represented by metal and dielectric bonds of a cubic lattice. After such discretization, Eq. (4) acquires the form of Kirchhoff's equations defined on a cubic lattice.[7] We write the Kirchhoff's equations in terms of the local dielectric constant and assume that the external electric field $\mathbf{E}_0$ is directed along "z" axis. Thus we obtain the following set of equations

$$\sum_j \epsilon_{ij}(\phi_j-\phi_i)=\sum_j \epsilon_{ij}E_{ij}, \tag{5}$$

where ϕ_i and ϕ_j are the electric potentials determined at the sites of the cubic lattice and the summation is over the nearest neighbors of the site i. The electromotive force (EMF) E_{ij} takes value E_0a_0, for the bond $\langle ij\rangle$ in the positive z direction (where a_0 is the spatial period of the cubic lattice) and $-E_0a_0$, for the bond $\langle ij\rangle$ in the $-z$ direction; $E_{kj}=0$ for the other four bonds at the site i. Thus, the composite is modeled by a resistor-capacitor-inductor network represented by Kirchhoff's Eq. (5). The EMF forces E_{ij} represent the external electric field applied to the system. In transition from the continuous medium described by Eq. (3) to the random network described by Eq. (5) we suppose, as usually,[7,15,35] that bond permittivities ϵ_{ij} are statistically independent and set a_0 to be equal to the metal grain size, $a_0=a$. In the considered case of two component metal-dielectric random composite, the permittivities ϵ_{ij} take values ϵ_m and ϵ_d, with probabilities p and $1-p$, respectively. Assuming that the bond permittivities ϵ_{ij} in Eq. (5) are statistically independent, we considerably simplify computer simulations as well as analytical consideration of local optical fields in the com-

posite. We note that important critical properties are universal, i.e., they are independent of details of a model, e.g., possible correlation of permittivities ϵ_{ij} in different bonds.

For further consideration we assume that the cubic lattice has a very large but finite number of sites N and rewrite Eq. (5) in matrix form with the "Hamiltonian" $\hat{H}$ defined in terms of the local dielectric constants,

$$\hat{H}\phi=\mathcal{E}, \tag{6}$$

where ϕ is a vector of the local potentials $\phi=\{\phi_1,\phi_2,\ldots,\phi_N\}$ determined in all N sites of the lattice, vector $\mathcal{E}$ equals to $\mathcal{E}_i=\Sigma_j\epsilon_{ij}E_{ij}$, as it follows from Eq. (5). The Hamiltonian $\hat{H}$ is $N\times N$ matrix that has off-diagonal elements $H_{ij}=-\epsilon_{ij}$ and diagonal elements defined as $H_{ii}=\Sigma_j\epsilon_{ij}$, where j refers to nearest neighbors of site i. The off-diagonal elements H_{ij} take values $\epsilon_d>0$ and $\epsilon_m=(-1+i\kappa)|\epsilon'_m|$ with probability p and $1-p$, respectively. The loss factor $\kappa=\epsilon''_m/|\epsilon'_m|$ is small, $\kappa\ll 1$. The diagonal elements H_{ii} are distributed between $2d\epsilon_m$ and $2d\epsilon_d$, where d is the dimensionality of the space ($2d$ is the number of the nearest neighbors in d-dimensional cubic lattice).

It is convenient to represent the Hamiltonian $\hat{H}$ as a sum of two Hermitian Hamiltonians $\hat{H}=\hat{H}'+i\kappa\hat{H}''$, where the term $i\kappa\hat{H}''$ ($\kappa\ll 1$) represents losses in the system. The Hamiltonian $\hat{H}'$ formally coincides with the Hamiltonian of the problem of metal-insulator transition (Anderson transition) in quantum systems.[41–44] More specifically, the Hamiltonian $\hat{H}'$ maps the quantum-mechanical Hamiltonian for the Anderson transition problem with both on- and off-diagonal correlated disorder. Since the off-diagonal matrix elements in $\hat{H}'$ have different signs, the Hamiltonian is similar to the so-called gauge-invariant model. This model, in turn, is a simple version of the random flux model, which represents a quantum system with random magnetic field[41] (see also recent numerical studies[45–47]). Hereafter, we refer to operator $\hat{H}'$ as to Kirchhoff's Hamiltonian (KH).

Thus, the problem of the field distribution in the system, i.e., the problem of finding solution to Kirchhoff's Eq. (5) or (6), becomes the eigenfunction problem for the KH, $\hat{H}'\Psi_n=\Lambda_n\Psi_n$, whereas the losses can be treated as perturbation. Since the real part ϵ'_m of metal dielectric function ϵ_m is negative, $\epsilon'_m<0$, and the permittivity of dielectric host is positive, $\epsilon_d>0$, the manifold of the KH eigenvalues Λ_n contains eigenvalues that have the real parts equal (or close) to zero. Then eigenstates Ψ_n that correspond to eigenvalues $|\Lambda_n/\epsilon_m|\ll 1$ are strongly excited by the external field and seen as giant field fluctuations, representing the resonant sp modes. If we assume that the eigenstates excited by the external field are localized, they should look like local-field peaks. The average distance between the field peaks can be estimated as $a(N/n)^{1/d}$, where n is the number of the KH eigenstates excited by the external field and N is the total number of the eigenstates.

Now we consider in more detail behavior of the eigenfunctions Ψ_n of the HK $\hat{H}'$, in the special case when $\epsilon'_m=-\epsilon_d$, corresponding the plasmon resonance of individual particles in a $2d$ system. Since a solution to Eq. (5) does not change when multiplying ϵ_m and ϵ_d by the same factor, we can normalize the system and set $\epsilon_d=-\epsilon_m=1$.

According to the one-parameter scaling theory the eigenstates Ψ_n are all localized for the $2d$ case (see, however, discussion in Refs. 44 and 48). On the other hand, it was shown in computer simulations[49] that there is a transition from chaotic[50,51] to localized eigenstates for the $2d$ Anderson problem,[49] with an intermediate crossover region. We consider first the case when metal concentration p is equal to the percolation threshold $p_c=1/2$ for the $2d$ bond percolating problem. Then the on-diagonal disorder in the KH $\hat{H}'$ is characterized by $\langle H'_{ii}\rangle=0$, $\langle H'^2_{ii}\rangle=4$ that corresponds to the chaos-localization transition.[49] The KH has also strong off-diagonal disorder, $\langle H'_{ij}\rangle=0$ $(i\neq j)$, which favors localization.[45,46] Our conjecture is that eigenstates Ψ_n are localized for all Λ_n in the $2d$ system. (We cannot rule out a possibility of inhomogeneous localization, similar to that obtained for fractals,[52] or the power-law localization;[41,53] note, however, that these possibilities are in strong disagreement with the one-parameter scaling theory).

In the considered case of $\epsilon_d=-\epsilon_m=1$ and $p=1/2$, all parameters in the KH $\hat{H}'$ are of the order of unity and its properties do not change under the transformation $\epsilon_d\Leftrightarrow\epsilon_m$. Therefore, the real eigenvalues Λ_n are distributed symmetrically with respect to zero, in an interval of the order of one. The eigenstates with $\Lambda_n\approx 0$ are effectively excited by the external field and represent the giant local-field fluctuations. When metal concentration p decreases (increases), the eigenstates with $\Lambda_n\approx 0$ are shifted from the center of the distribution toward its lower (upper) edge, which typically favors localization. Because of this, we assume that the eigenstates, or at least those with $\Lambda_n\approx 0$, are localized, for all metal concentrations p in the $2d$ case.

Despite the great effort and all the progress made, the Anderson transition is not yet fully understood in the $3d$ case and very little is known about the eigenfunctions of the Anderson Hamiltonian, even in the case of a diagonal disorder only.[41–44,54] We mention here recent computer simulations[47] for a $3d$ system similar to our system with $\epsilon_d=-\epsilon_m=1$, $p=1/2$. The authors of Ref. 46 investigate the Anderson problem with diagonal-matrix elements w_{ii} distributed uniformly around zero $-w_0/2\leq w_{ii}\leq w_0/2$ and off-diagonal elements $t_{ij}=\exp(i\phi_{ij})$, with phases ϕ_{ij} also distributed uniformly $0\leq\phi_{ij}\leq 2\pi$. It was found that in the center of the band, the states are localized for the disorder $w_0>w_c=18.8$. In our $3d$ HK $\hat{H}'$ Hamiltonian, the diagonal elements are distributed as $-6\leq H_{ii}\leq 6$ and, therefore, the diagonal disorder is smaller than the above critical disorder w_c. On the other hand, our off-diagonal disorder is stronger than in calculations.[46] It is shown[44,45] that even small off-diagonal disorder strongly enforces localization. We conjecture here that the eigenstates corresponding to the eigenvalues $\Lambda_n\approx 0$ in the $3d$ case are also localized for all p.

Suppose we found all eigenvalues Λ_n and eigenfunctions Ψ_n of $\hat{H}'$. Then we can express the potential ϕ in Eq. (6) in terms of the eigenfunctions as $\phi=\Sigma_n A_n\Psi_n$ and substitute it in Eq. (6). Thus, we obtain the following equation for coefficients A_n:

$$(i\kappa b_n+\Lambda_n)A_n+i\kappa\sum_{m\neq n}(\Psi_n|\hat{H}''|\Psi_m)A_m=\mathcal{E}_n, \quad (7)$$

where $b_n=(\Psi_n|\hat{H}''|\Psi_n)$, and $\mathcal{E}_n=(\Psi_n|\mathcal{E})$ is a projection of the external field on eigenstate Ψ_n. (The product of two vectors, e.g., Ψ_n and $\mathcal{E}$ is defined here in a usual way, as $\mathcal{E}_n=(\Psi_n|\mathcal{E})\equiv\Sigma_i\Psi^*_{n,i}\mathcal{E}_i$, where the sum is over all lattice sites). Since all parameters in the real Hamiltonian $\hat{H}''$ are of the order of unity, the matrix elements b_n are also of the order of unity. We approximate them by some constant b, which is about unity. We suggest that eigenstates Ψ_n are localized within spatial domains $\xi_A(\Lambda)$, where $\xi_A(\Lambda)$ is the Anderson localization length, which depends on Λ. Then, the sum in Eq. (7) converges and it can be treated as a small perturbation. In the zeroth approximation,

$$A_n^{(0)}=\mathcal{E}_n/(\Lambda_n+i\kappa b_n). \quad (8)$$

The first-order correction to A_n is equal to

$$A_n^{(1)}=-i\kappa\sum_{m\neq n}(\Psi_n|\hat{H}''|\Psi_m)\mathcal{E}_m/(\Lambda_m+i\kappa b_m). \quad (9)$$

For $\kappa\to 0$, most important eigenstates in this sum are those with $|\Lambda_m|\leq b\kappa$. Since the eigenstates Λ_n are distributed in the interval of the order of unity the spatial density of the eigenmodes with $|\Lambda_m|\leq b\kappa$ vanishes as $a^{-d}\kappa\to 0$ at $\kappa\to 0$. Therefore, $A_n^{(1)}$ is exponentially small $|A_n^{(1)}|\sim|\Sigma_{m\neq n}(\Psi_n|\hat{H}''|\Psi_m)\mathcal{E}_m/b_m|\propto\exp\{-[a/\xi_A(0)]\kappa^{-1/d}\}$ and can be neglected when $\kappa\ll[a/\xi_A(0)]^d$. Then, the local potential ϕ is equal to $\phi(\mathbf{r})=\Sigma_n A_n^{(0)}\Psi_n=\Sigma_n\mathcal{E}_n\Psi_n(r)/(\Lambda_n+i\kappa b)$ [see Eq. (8)] and the fluctuating part of the local field $\mathbf{E}_f=-\nabla\phi(\mathbf{r})$ is given by

$$\mathbf{E}_f(\mathbf{r})=-\sum_n\mathcal{E}_n\nabla\Psi_n(\mathbf{r})/(\Lambda_n+i\kappa b). \quad (10)$$

The average field intensity is as follows:

$$\langle|E|^2\rangle=\langle|\mathbf{E}_f+\mathbf{E}_0|^2\rangle=E_0^2+\left\langle\sum_{n,m}\frac{\mathcal{E}_n\mathcal{E}^*_m[\nabla\Psi_n(\mathbf{r})\cdot\nabla\Psi^*_m(\mathbf{r})]}{(\Lambda_n+i\kappa b)(\Lambda_m-i\kappa b)}\right\rangle, \quad (11)$$

where we took into account that $\langle\mathbf{E}_f\rangle=\langle\mathbf{E}_f^*\rangle=0$. We consider now the eigenstates Ψ_n with eigenvalues Λ_n within a small interval $|\Lambda_n-\Lambda|\leq\Delta\Lambda\ll\kappa$ centered at Λ. These states are denoted as $\Psi_n(\Lambda,\mathbf{r})$. Recall that the eigenstates are assumed to be localized so that eigenfunctions $\Psi_n(\Lambda,\mathbf{r})$ are well separated in space. The average distance between them, l, can be estimated as $l(\Delta\Lambda)\sim a[\rho(\Lambda)\Delta\Lambda]^{-1/d}$, where

$$\rho(\Lambda)=a^d\sum_n\delta(\Lambda-\Lambda_n)/V \quad (12)$$

is the dimensionless density of states for the KH $\hat{H}'$ and V is the volume of the system. We assume here that the metal concentration p is about one half so that all quantities in the KH $\hat{H}'$ are about unity and, therefore, the density of states $\rho(\Lambda)$ is also about unity at the center of the spectrum, i.e., at $\Lambda=0$. Then the distance $l(\Delta\Lambda)$ can be arbitrary large for $\Delta\Lambda\to 0$; we assume, of course, that $l(\Delta\Lambda)$ is still much smaller than the system size, and the total number of eigenstates $\Psi_n(\Lambda,\mathbf{r})$ is macroscopically large. When the interstate distance $l(\Delta\Lambda)$ is much larger than the localization length $\xi_A(\Lambda)$ the localized eigenfunctions $\Psi_n(\Lambda,\mathbf{r})$ can be characterized by special positions of their "centers" $\mathbf{r}_n$ so that $\Psi_n(\Lambda,\mathbf{r})=\Psi(\Lambda,\mathbf{r}-\mathbf{r}_n)$ and Eq. (11) acquires the following form:

$$\langle|E|^2\rangle=E_0^2+\sum_{\Lambda_1,\Lambda_2}\times\frac{\left\langle\sum_{n,m}\mathcal{E}_n\mathcal{E}^*_m[\nabla\Psi(\Lambda_1,\mathbf{r}-\mathbf{r}_n)\cdot\nabla\Psi^*(\Lambda_2,\mathbf{r}-\mathbf{r}_m)]\right\rangle}{(\Lambda_1+i\kappa b)(\Lambda_2-i\kappa b)}, \quad (13)$$

where the first sum is over positions of the intervals $|\Lambda_n-\Lambda_1|$ and $|\Lambda_m-\Lambda_2|$ in the Λ space, whereas the sum in the numerator is over spatial positions $\mathbf{r}_n$ and $\mathbf{r}_m$ of the eigenfunctions. For each realization of a macroscopically homogeneous random film, the positions $\mathbf{r}_n$ of eigenfunctions $\Psi(\Lambda,\mathbf{r}-\mathbf{r}_n)$ take new values that do not correlate with the value of Λ. Therefore, we can independently average the numerator in the second term of Eq. (13) over positions $\mathbf{r}_n$ and $\mathbf{r}_m$ of eigenstates Ψ_n and Ψ_m. Taking into account that $\langle\nabla\Psi_n(\mathbf{r})\rangle=0$, we obtain

$$\langle\mathcal{E}_n\mathcal{E}^*_m[\nabla\Psi(\Lambda_1,\mathbf{r}-\mathbf{r}_n)\cdot\nabla\Psi^*(\Lambda_2,\mathbf{r}-\mathbf{r}_m)]\rangle\simeq\langle|\mathcal{E}_n|^2|\nabla\Psi(\Lambda_1,\mathbf{r}-\mathbf{r}_n)|^2\rangle\delta_{\Lambda_1\Lambda_2}\delta_{nm}, \quad (14)$$

where we neglected possible correlations of eigenfunctions from different intervals Λ_1 and Λ_2 since the spatial density of the eigenfunctions excited effectively by the external field is estimated as $a^{-d}\rho(\Lambda)\kappa$, i.e., it vanishes for $\kappa\to 0$. Substitution of Eq. (14) in Eq. (11) results in

$$\langle|E|^2\rangle=E_0^2+\sum_\Lambda\frac{\sum_n|\mathcal{E}_n|^2\langle|\nabla\Psi_n(\Lambda,\mathbf{r})|^2\rangle}{\Lambda^2+(b\kappa)^2}. \quad (15)$$

The localized eigenstates are not, in general, degenerate, so that the eigenfunctions Ψ_n can be chosen as real. Then we can estimate $|\mathcal{E}_n|^2=|(\Psi_n|\mathcal{E})|^2=|\Sigma_{i=1}^N\Psi_{n,i}\mathcal{E}_i|^2$ in Eq. (15) by replacing the sum over all N sites of the system with integration over the system volume V, which gives $|\mathcal{E}_n|^2\sim a^{-2d}|\int\Psi_n\mathcal{E}d\mathbf{r}|^2$. Using Eqs. (5) and (4), we find

$$|\mathcal{E}_n|^2\sim a^{4-2d}\left|\int\Psi_n(\mathbf{E}_0\cdot\nabla\epsilon)d\mathbf{r}\right|^2=a^{4-2d}\left|\int\epsilon(\mathbf{E}_0\cdot\nabla\Psi_n)d\mathbf{r}\right|^2, \quad (16)$$

where to obtain the last relation we integrated by parts and took into account that the eigenstates Ψ_n are localized within the localization length $\xi_A(\Lambda)$. Since the local dielectric constant $|\epsilon|$ are of the order of unity, $|\epsilon|\sim 1$, and the spatial derivative $\nabla\Psi_n$ is estimated as $\Psi_n/\xi_A(\Lambda)$ in Eq. (16) we find

$$|\mathcal{E}_n|^2 \sim \frac{E_0^2 a^4}{a^{2d}\xi_A^2(\Lambda)}\left|\int \Psi_n(\mathbf{r})d\mathbf{r}\right|^2 \sim \frac{E_0^2 a^4}{\xi_A^2(\Lambda)}\left|\sum_{i=1}^{N}\Psi_{n,i}\right|^2, \tag{17}$$

where we returned back to summation over sites of the tight-binding model. Since the eigenfunctions Ψ_n are normalized to unity, i.e., $\langle\Psi_n|\Psi_n\rangle=\Sigma_{i=1}^{N}|\Psi_{n,i}|^2=1$ and localized within $\xi_A(\Lambda)$ we estimate them as $\Psi_{n,i}\sim[\xi_A(\Lambda)/a]^{-d/2}$ in the localization domain. Substituting this estimate in Eq. (17) we obtain

$$|\mathcal{E}_n|^2 \sim E_0^2 a^2[\xi_A(\Lambda)/a]^{d-2}. \tag{18}$$

In a similar way we can estimate the average spatial derivative in the numerator of Eq. (15),

$$\begin{aligned}\langle|\nabla\Psi_n(\Lambda,\mathbf{r})|^2\rangle &\sim \xi_A^{-2}(\Lambda)\langle|\Psi_n(\Lambda,\mathbf{r})|^2\rangle \\ &\sim \xi_A^{-2}(\Lambda)N^{-1}\sum_{i=1}^{N}|\Psi_{n,i}|^2 \\ &\sim \xi_A^{-2}(\Lambda)/N,\end{aligned} \tag{19}$$

where $N=V/a^d$ is the total number of sites. Now we use the estimates (18) and (19) and rewrite the numerator of Eq. (15) as

$$\begin{aligned}\sum_n |\mathcal{E}_n|^2\langle|\nabla\Psi_n(\Lambda,\mathbf{r})|^2\rangle &\sim \frac{1}{N}\sum_n E_0^2[\xi_A(\Lambda)/a]^{d-4} \\ &\sim E_0^2[\xi_A(\Lambda)/a]^{d-4}\rho(\Lambda)\Delta\Lambda,\end{aligned} \tag{20}$$

where we took into account that the total number of the eigenstates within interval $\Delta\Lambda$ is equal to $N\rho(\Lambda)\Delta\Lambda$. By substituting Eq. (20) in Eq. (15) and replacing the summation by integration over Λ, we obtain the following estimate for the field intensity

$$\langle|E|^2\rangle \sim E_0^2 + E_0^2\int \frac{\rho(\Lambda)[a/\xi_A(\Lambda)]^{4-d}}{\Lambda^2+(b\kappa)^2}d\Lambda. \tag{21}$$

Since all matrix elements in KH H′ are of the order of unity (in fact, the off-diagonal elements are ± 1), the density of states $\rho(\Lambda)$ and localization length $\xi_A(\Lambda)$ change significantly within an interval of an order of one. In contrast, the denominator in Eq. (15) has an essential singularity at $\Lambda=\pm ib\kappa$. Then the second moment of the local-electric field $M_2\equiv M_{2,0}=\langle|E|^2\rangle/E_0^2$ is estimated as

$$\begin{aligned}M_2^* &\sim 1+\rho(a/\xi_A)^{4-d}\int\frac{1}{\Lambda^2+(b\kappa)^2}d\Lambda \\ &\sim \rho(a/\xi_A)^{4-d}\kappa^{-1}\gg 1,\end{aligned} \tag{22}$$

provided that $\kappa\ll\rho(a/\xi_A)^{4-d}$ [we set $\xi_A(\Lambda=0)\equiv\xi_A$, $\rho(\Lambda=0)\equiv\rho$ and approximated b by unity]. Thus, the field distribution, in this case, can be described as a set of the KH eigenstates localized within ξ_A, with the field peaks having the amplitudes

$$E_m^* \sim E_0\kappa^{-1}(a/\xi_A)^2, \tag{23}$$

which are separated in distance by the field correlation length

$$\xi_e^* \sim a(\rho\kappa b)^{-1/d} \sim a(\rho\kappa)^{-1/d}, \tag{24}$$

where again we used that $b\sim 1$. All the above speculations leading to Eqs. (22)–(24) hold when the field correlation length ξ_e^* is much larger than the Anderson localization length, i.e., $\xi_e^*\gg\xi_A$. This condition is fulfilled in the limit of small losses when $\kappa\to 0$.

Note that hereafter by the superscript * we mark the quantities, which are given for the special case $-\epsilon_m=\epsilon_d=1$ considered here. (The sign *, of course, should not be confused with complex conjugation denoted by *.) Using the scale renormalization described in the next subsection, we will see how these quantities are transformed when $|\epsilon_m/\epsilon_d|\gg 1$, i.e., in the long wavelength part of the spectrum. Note also that, for ξ_A and ρ we omit the * sign in order to avoid complicated notations; it is implied that their values are always taken at $-\epsilon_m=\epsilon_d=1$, even if the case of $|\epsilon_m/\epsilon_d|\gg 1$ is considered.

In the above estimates we supposed that the localization length ξ_A is proportional to the eigenstate "size." This assumption might not be exact for the Anderson system, in general (e.g., see discussion in Ref. 41), but it is confirmed well by our numerical calculations (see Figs. 1 and 2 and Figs. 2 and 3 in Ref. 10) for the case of $2d$ percolation composites.

The above results for the field distribution are in good agreement with comprehensive numerical calculations performed in Refs. 27, 28, 29 for a $2d$ system with $\epsilon_m/\epsilon_d\approx -1$ and $p=p_c=1/2$. It was shown there that the average intensity of the local field fluctuations, i.e., the second moment M_2^* is estimated as $M_2^*\sim\kappa^{-\gamma}$, where the critical exponent $\gamma\approx 1.0$. The authors also found that the correlation length ξ_e^* of the field fluctuations diverges as $\xi_e^*\sim\kappa^{-\nu_e}$ at $\kappa\to 0$, where the critical exponent $\nu_e\approx 0.5$. For $d=2$, these values of γ and ν_e are very close to $\gamma=1$ and $\nu_e=1/2$ found here.

Above we assumed that metal concentration p is about one half, which corresponds to the percolation threshold for $d=2$. The derivation of Eqs. (21) and (22) was based on the assumption that the density of states $\rho(\Lambda)$ is finite and about unity for $\Lambda=0$. This assumption, however, is violated for small metal concentration p, when the eigenvalue distribution shifts to the positive side of Λ, so that the eigenstates with $\Lambda\approx 0$ are shifted to the lower edge of the distribution. Then, the density of states ρ in Eq. (22) becomes a function of the metal concentration p. In the limit of $p\to 0$, the number of states effectively excited by the external field is proportional to the number of metal particles. Then the function $\rho(p)$ can be estimated as $\rho(p)\sim p$, for $p\to 0$. The same consideration holds in the other limit, when a small portion of holes in otherwise continuous film resonate with the external field and the density of states can be estimated as $\rho(p)\sim 1-p$, for $p\to 1$. When the density of states decreases, localization becomes stronger and we estimate the localization length ξ_A as $\xi_A(\Lambda=0,p\to 0)\sim\xi_A(\Lambda=0,p\to 1)\sim a$. It follows then from Eq. (22) that strong field fluctuations ($M_2>1$) exist in a metal-dielectric composite with $\epsilon_d=-\epsilon_m'$ in the wide concentration range

$$\kappa<p<1-\kappa, \quad \kappa\ll 1. \tag{25}$$

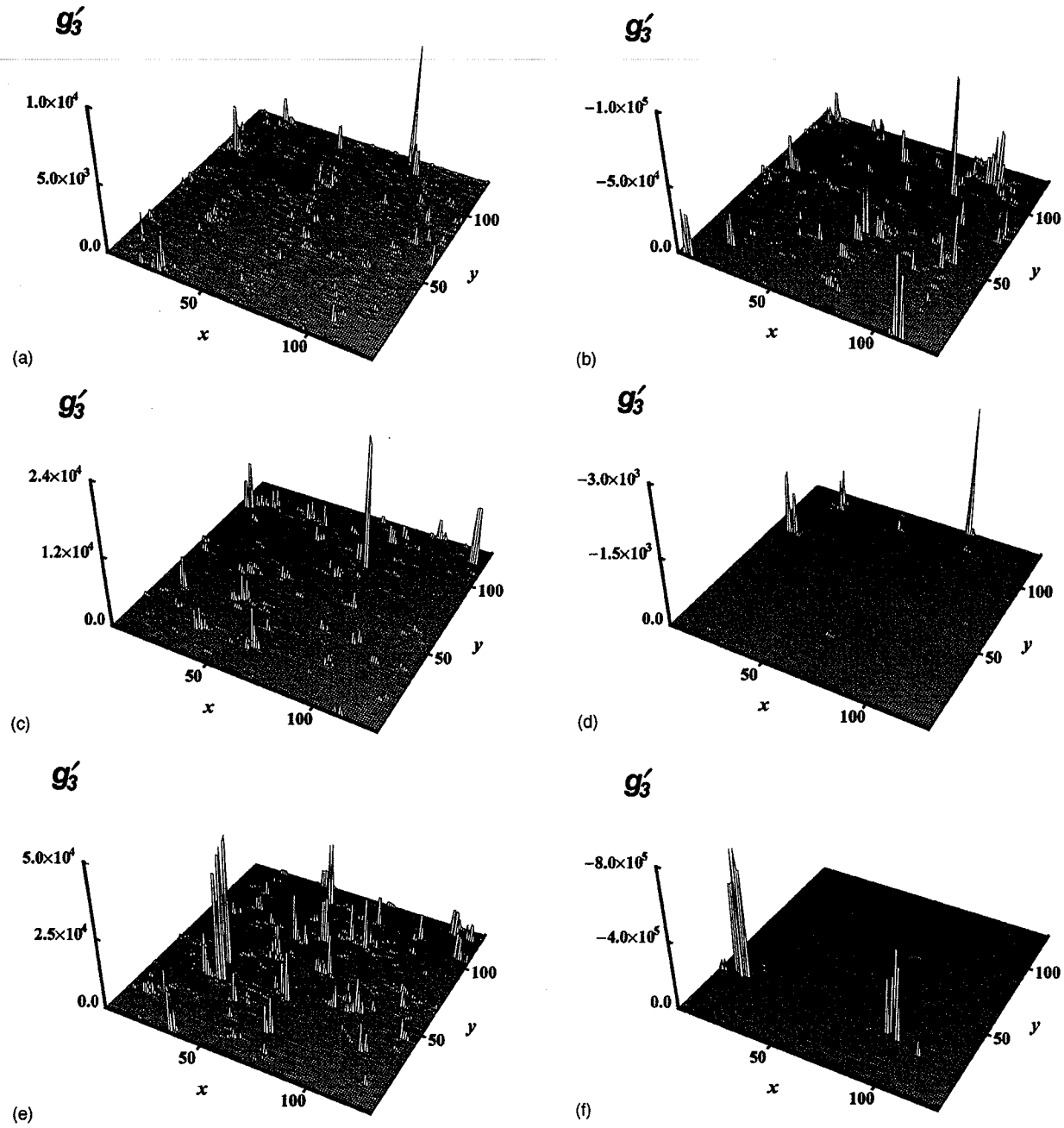

FIG. 1. Distribution of x component of local "THG field source" (real part) $g_3'=\mathrm{Re}[E^2(\mathbf{r})E_x(\mathbf{r})]$ in semicontinuous silver films at wavelength $\lambda=1.5$ μm, for different metal concentration p. (a) and (b): $p=0.3$; (c) and (d): $p=p_c=0.5$; (e) and (f): $p=0.7$. The positive [(a), (c), (e)] and negative [(b), (d), (f)] values of the local nonlinear fields are shown in different figures. The applied field $E_0=1$.

Although we estimated above local fields for the special case of $\epsilon_d=-\epsilon_m'$ all the above speculations, which are based on the assumption that the eigenstates of KH are localized, hold in a more general case, when the real part of the metal dielectric constant ϵ_m' is negative and its absolute value is of the order of ϵ_d. The important case of the large contrast when $|\epsilon_m|\gg\epsilon_d$ will be considered in the next subsection.

Note that the above speculations leading to prediction of giant field fluctuations described by Eqs. (21) and (22), do not require long-range spatial correlations (such, for example, as in fractal structures) in particle positions. The large field fluctuations have been seen in computer simulations, in particular, for the so-called random gas of metal particle,[55,56] i.e., for metal particles randomly distributed in space. This, however, is not true when the contrast is large $|\epsilon_m|\gg\epsilon_d$; we show below that in this case the internal structure of a composite becomes crucial.

To get a further insight in the optical field distribution in percolation metal-dielectric composites, we employ the original idea for computer simulations described in details in our previous publications[27–31] and calculate the local electric field distribution for a two-dimensional percolation composite (see Figs. 1 and 2). We model a film by a square lattice consisting of metallic bonds, with the conductivity $\sigma_m=$

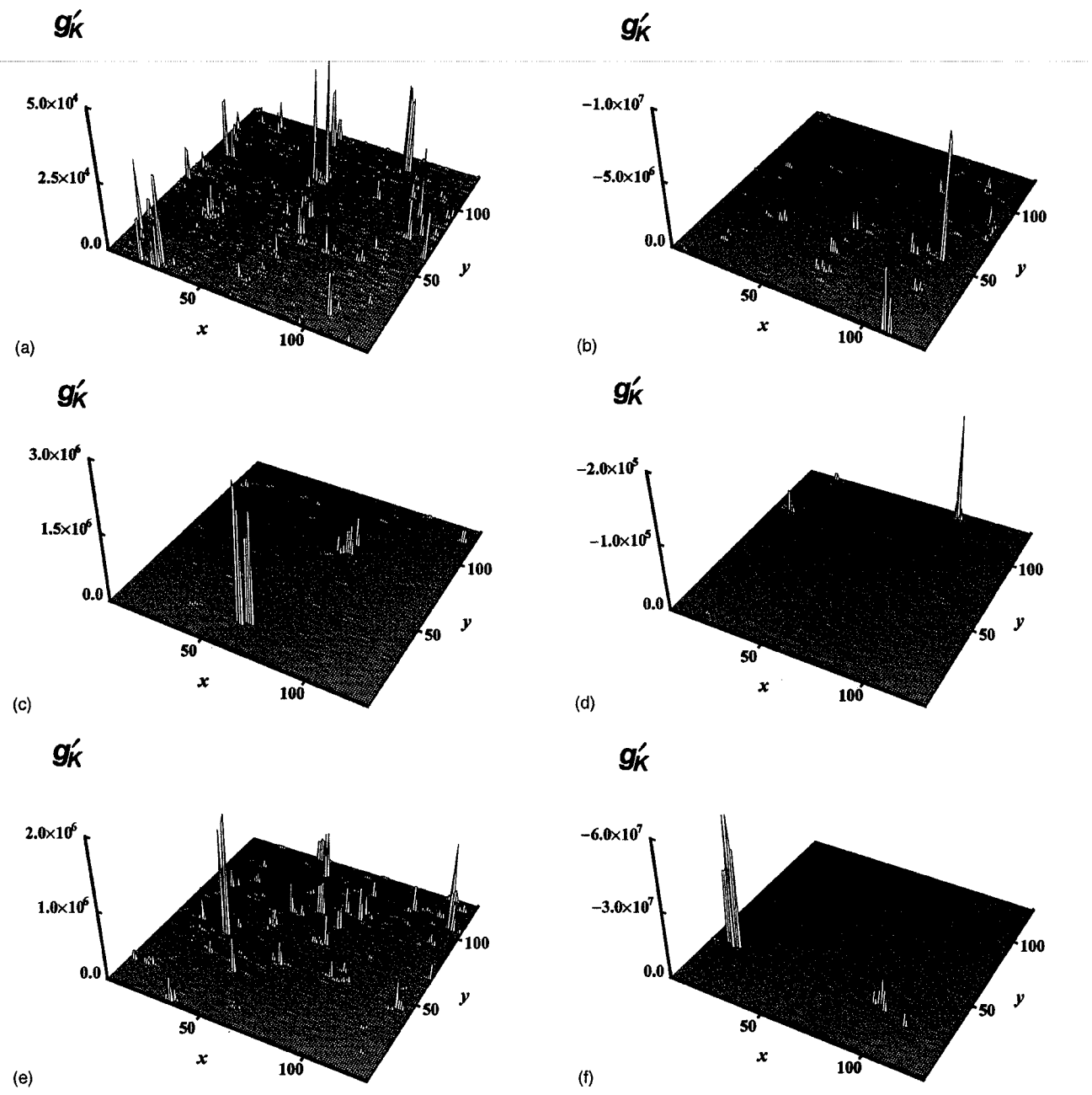

FIG. 2. Distribution of local "Kerr field" (real part) $g'_K = \mathrm{Re}[E^2(\mathbf{r})|E(\mathbf{r})|^2]$ in semicontinuous silver films at wavelength $\lambda = 1.5$ μm, for different metal concentration p. (a) and (b): $p = 0.3$; (c) and (d): $p = p_c = 0.5$; (e) and (f): $p = 0.7$. The positive [(a), (c), (e)] and negative [(b), (d), (f)] values of the local fields are shown in different figures. The applied field $E_0 = 1$.

$-i\epsilon_m\omega/4\pi$ (L-R bonds) and concentration p, and dielectric bonds with the conductivity $\sigma_d = -i\epsilon_d\omega/4\pi$ and concentration $1-p$ (C bonds). The amplitude of the incident wave $E_0 \equiv E^{(0)}$ (for the applied field we use interchangeably the notations E_0 and $E^{(0)}$) is set equal one, $E_0 = 1$, whereas the local fields inside the system are complex quantities. The calculations are performed for silver-on-glass film. The dielectric constant of silver has the form of Eq. (1), with the interband-transitions contribution $\epsilon_b = 5.0$, plasma frequency $\omega_p = 9.1$ eV, and relaxation rate $\omega_\tau = 0.021$ eV.[57] We also used $\epsilon_d = 2.2$ for a glass host. In Fig. 1, as an example, we show the distribution for the local field product $g'_3(\mathbf{r}) = \mathrm{Re}[E^2(\mathbf{r})E_x(\mathbf{r})]/|E^{(0)}|^3$, for wavelength $\lambda = 1.5$ μm, which corresponds to $\epsilon_m \approx -118 + i3.2$ (three different concentrations, $p = 0.3$, $p = p_c = 0.5$, and $p = 0.7$ were used in simulations). The quantity $g_3(\mathbf{r})$ determines the local nonlinear source (polarization) for third-harmonic generation, third-harmonic generation (THG) (see Section III). In Fig. 2, we also show the local field product $g'_K(\mathbf{r}) = \mathrm{Re}[E^2(\mathbf{r})|E(\mathbf{r})|^2]/|E^{(0)}|^4$ for the same parameters $\lambda = 1.5$ μm, $p = 0.3$, $p = p_c = 0.5$, and $p = 0.7$ of the silver semicontinuous film. The integral of $g_K(\mathbf{r})$ determines the average enhancement for the Kerr nonlinearity. For simplicity, all the distances in Figs. 1 and 2 are given in a units. As

seen in the figures, the fluctuating nonlinear fields are well localized. They form a set of peaks with the magnitudes up to 10^6 for $g_3'(\mathbf{r})$ and up to 5×10^7 for $g_K'(\mathbf{r})$ that are different in sign; the peaks and their spatial separations become larger with further increase of λ (see also Fig. 3 in Ref. 10). Qualitatively similar distributions were obtained for the imaginary parts of $g_3(\mathbf{r})$ and $g_K(\mathbf{r})$ (not shown).

B. High-order moments of local electric fields

Now, we consider arbitrary high-order field moments defined as

$$M_{n,m}=\frac{1}{VE_0^m|E_0|^n}\int |E(\mathbf{r})|^n E^m(\mathbf{r})d\mathbf{r}, \tag{26}$$

where, as above, $E_0\equiv E^{(0)}$ is the amplitude of the external field and $E(\mathbf{r})$ [which is defined so that $E^2(\mathbf{r})\equiv\mathbf{E}(\mathbf{r})\cdot\mathbf{E}(\mathbf{r})$] is the amplitude of the local field; the integration is over the total volume V of a system.

The high-order field moment $\langle M_{2k,m}\propto E^{k+m}E^{*k}\rangle$ represents a nonlinear optical process in which in one elementary act $k+m$ photons are added and k photons are subtracted.[17] This is because the complex conjugated field in the general expression for the nonlinear polarization implies photon subtraction so that the corresponding frequency enters the nonlinear susceptibility with the negative sign.[17] Enhancement of the Kerr optical nonlinearity G_K is proportional to $M_{2,2}$, third-harmonic generation (THG) enhancement is given by $|M_{0,3}|^2$, and surface-enhanced Raman scattering (SERS) is represented by $M_{4,0}$ (see next section). Integrands in Eq. (26) for $M_{2,2}$ and $M_{0,3}$, i.e., the local nonlinear fields $g_3=|E(\mathbf{r})|^2E(\mathbf{r})/(E_0|E_0|^2)$ and $g_K=|E(\mathbf{r})|^2E^2(\mathbf{r})/(E_0^2|E_0|^2)$ are shown in Figs. 1 and 2.

We are interested here in the case when $M_{n,m}\gg1$, which implies that the fluctuating part of the local electric field $\mathbf{E}_f$ is much larger than the applied field $\mathbf{E}_0$. We substitute in Eq. (26) the expression for $\mathbf{E}_f$ given by Eq. (10) and obtain for the moment $M_{2p,2q}$ (p and q are integers) the following equation

$$M_{2p,2q}=\Bigg\langle\sum_{n_1,n_2,\cdots n_{2p};m_1,m_2,\cdots m_{2q}}^{N}\frac{\mathcal{E}_{n_1}\mathcal{E}_{n_2}(\nabla\Psi_{n_1}\cdot\nabla\Psi_{n_2}^*)\cdots\mathcal{E}_{n_{2p-1}}\mathcal{E}_{n_{2p}}(\nabla\Psi_{n_{2p-1}}\cdot\nabla\Psi_{n_{2p}}^*)}{(\Lambda_{n_1}+ibk)(\Lambda_{n_2}-ibk)\cdots(\Lambda_{n_{2p-1}}+ibk)(\Lambda_{n_{2p}}-ibk)}$$
$$\times\frac{\mathcal{E}_{m_1}\mathcal{E}_{m_2}(\nabla\Psi_{m_1}\cdot\nabla\Psi_{m_2})\cdots\mathcal{E}_{m_{2q-1}}\mathcal{E}_{m_{2q}}(\nabla\Psi_{m_{2q-1}}\cdot\nabla\Psi_{m_{2q}})}{(\Lambda_{m_1}+ibk)(\Lambda_{m_2}+ibk)\cdots(\Lambda_{m_{2q-1}}+ibk)(\Lambda_{m_{2q}}+ibk)}\Bigg\rangle, \tag{27}$$

where $\langle\cdots\rangle$ denotes as above the ensemble average, which is equivalent to the volume average and the sums are over all eigenstates of KH $\hat{H}'$. As a next step, we average Eq. (27) over spatial positions of eigenstates $\Psi_n(\mathbf{r})\equiv\Psi(\mathbf{r}-\mathbf{r}_n)$ as it has been done in transition from Eq. (13) to Eq. (15); this results in the following estimate

$$M_{2p,2q}\sim\sum_{\Lambda}\frac{\sum_{|\Lambda_n-\Lambda|\le\Delta\Lambda}|\mathcal{E}_n|^{2p}\mathcal{E}_n^{2q}\langle(\nabla\Psi_n\cdot\nabla\Psi_n^*)^p(\nabla\Psi_n\cdot\nabla\Psi_n)^q\rangle}{(\Lambda^2+(bk)^2)^p(\Lambda+ibk)^{2q}}, \tag{28}$$

where the summation in the numerator is over eigenfunctions $\Psi_n=\Psi(\Lambda,\mathbf{r}-\mathbf{r}_n)$ with eigenvalues within the interval $|\Lambda_n-\Lambda|\le\Delta\Lambda\ll\kappa$, while the external sum is over positions Λ of the intervals that cover the whole range of eigenvalues Λ_n. The average in the numerator of Eq. (28) can be estimated as follows [see derivation of Eq. (19)]

$$\langle(\nabla\Psi_n\cdot\nabla\Psi_n^*)^p(\nabla\Psi_n\cdot\nabla\Psi_n)^q\rangle$$
$$\sim\frac{1}{N\xi_A^{2(p+q)}(\Lambda)}\sum_{i=1}^{N}|\Psi_{n,i}|^{2p}\Psi_{n,i}^{2q}$$
$$\sim\frac{1}{N\xi_A^{2(p+q)}(\Lambda)}\left[\frac{a}{\xi_A}\right]^{d(p+q-1)}, \tag{29}$$

where, as above, $\xi_A(\Lambda)$ is the localization length, a is the period of the square lattice in the tight-binding model [see discussion after Eq. (5)], and N is the total number of cites in the lattice. We substitute this equation and expression for $\mathcal{E}_n$ given by Eq. (18) in Eq. (28). Then the sum in the numerator of Eq. (28) takes the following form

$$\sum_{|\Lambda_n-\Lambda|\le\Delta\Lambda}|\mathcal{E}_n|^{2p}\mathcal{E}_n^{2q}\langle(\nabla\Psi_n\cdot\nabla\Psi_n^*)^p(\nabla\Psi_n\cdot\nabla\Psi_n)^q\rangle$$
$$\sim\rho(\Lambda)[a/\xi_A(\Lambda)]^{4(p+q)-d}\Delta\Lambda, \tag{30}$$

where $\rho(\Lambda)$ is the dimensionless density of states [see Eq. (12)]. By replacing the first sum in Eq. (28) by integration over the spectrum we obtain

$$M_{2p,2q}\sim\int\frac{\rho(\Lambda)[a/\xi_A(\Lambda)]^{4(p+q)-d}}{[\Lambda^2+(b\kappa)^2]^p(\Lambda+ib\kappa)^{2q}}d\Lambda. \tag{31}$$

Note that to obtain the above expression we neglected all cross terms in the product of eigenstates, when averaging Eq. (27) over the spatial positions of the eigenfunctions $\Psi_n=\Psi(\Lambda,\mathbf{r}-\mathbf{r}_n)$. It can be shown that after integrating over

Λ, these cross terms result in negligible [in comparison with the leading term given by (31)] contribution to $M_{n,m}$, for $\kappa \to 0$.

Assuming that the density of states $\rho(\Lambda)$ and the localization length $\xi_A(\Lambda)$ are both smooth functions of Λ in the vicinity of zero and taking into account that all parameters of the KH $\hat{H}'$ for the case $\epsilon_d = -\epsilon_m' = 1$ are of the order one, we obtain the following estimate for the local-field moments

$$M_{n,m}^{\star} \sim \rho(p)[a/\xi_A(p)]^{2(n+m)-d} \kappa^{-n-m+1}, \qquad (32)$$

for $n+m>1$ and $m>0$, where we set for simplicity $b=1$. Note that the same estimate can be obtained by considering the local fields as a set of peaks (stretched over the distance ξ_A), with the magnitude $E_m^{\star}$ and the average distance $\xi_e^{\star}$ between the peaks given by Eqs. (23) and (24). Recall that the superscript * denotes physical quantities defined in the system with $\epsilon_d = -\epsilon_m' = 1$. In Eq. (32), we indicated explicitly the dependence of the density of states $\rho(p)$ and localization length $\xi_A(p)$ on the metal concentration p [as mentioned above $\rho(p)$ and $\xi_A(p)$ are always given at $\epsilon_d = -\epsilon_m' = 1$ and the sign * for them is omitted]. The notations $\rho(p)$ and $\xi_A(p)$ should be understood as $\rho(p) = \rho(p, \Lambda = 0)$ and $\xi_A(p) = \xi_A(p, \Lambda = 0)$, i.e., they are given at $\Lambda = 0$.

The Anderson localization length $\xi_A(\Lambda)$ has, typically, its maximum at the center of the Λ distribution.[46] When p departs from 1/2, the value $\Lambda = 0$ moves from the center of the Λ-distribution toward its wings, where the localization is typically stronger (i.e., ξ_A is less). Therefore, it is plausible to suggest that $\xi_A(p)$ reaches its maximum at $p = 1/2$ and decreases toward $p = 0$ and $p = 1$, so that the absolute value of the local-field moments may have a minimum at $p = 1/2$, according to Eq. (32). In $2d$ composites the percolation threshold p_c is typically close to $p_c \simeq 0.5$. Therefore, the moments $M_{n,m}$ in $2d$ composites have a local minimum at the percolation threshold as a function of the metal concentration p. In accordance with this, the amplitudes of various nonlinear processes, while much enhanced, have a characteristic minimum at the percolation threshold [see Sec. III, Figs. (5) and (6)].

It is important to note that the moment magnitudes in Eq. (32) do not depend on the number of "subtracted" (annihilated) photons in one elementary act of the nonlinear scattering. If there is at least one such photon, then the poles in Eq. (31) are in different complex semiplanes and the result of the integration is estimated by Eq. (32).

However, for the case when all photons are added (in other words, all frequencies enter the nonlinear susceptibility with the sign plus), i.e., when $n = 0$, we cannot estimate the moments $M_{0,m} \equiv E_0^{-m} V^{-1} \int E^m(\mathbf{r}) d\mathbf{r}$ by Eq. (32) since the integral in Eq. (31) is not further determined by the poles at $\Lambda = \pm ib\kappa$. Yet all the functions of the integrand are about unity and the moment $M_{0,m}$ must be of the order of unity $M_{0,m} \sim O(1)$ for $m>1$. Note that the moment $M_{0,m}$ describes, in particular, enhancement G_{nHG} of n-order harmonic generation, through the relation $G_{nHG} = |M_{0,m}|^2$ (see Sec. III).

Above we assumed that $|\epsilon_m|/\epsilon_d \approx 1$. To estimate the local-field fluctuations in percolation composites for the large contrast, $|\epsilon_m|/\epsilon_d \gg 1$, we use the scaling approach developed in our previous paper[10] and generalize it for an arbitrary field moment. Here we recapitulate briefly the main points of the scaling renormalization. Consider first a percolation composite where the metal concentration p is equal to the percolation threshold, $p = p_c$. We divide a system into cubes of size l and consider each cube as a new renormalized element. All such cubes can be classified into two types. A cube that contains a continuous path of metallic particles is considered as a "conducting" element. A cube without such an "infinite" cluster is considered as a nonconducting, "dielectric," element.[59] The effective dielectric constant of the "conducting" cube $\epsilon_m(l)$ decreases with increasing its size l as $\epsilon_m(l) \simeq (l/a)^{-t/\nu} \epsilon_m$, whereas the effective dielectric constant of the "dielectric" cube $\epsilon_d(l)$ increases with l as $\epsilon_d(l) \simeq (l/a)^{s/\nu} \epsilon_d$ [t, s, and ν are the percolation critical exponents for the static conductivity, dielectric constant, and percolation correlation length, respectively; for $2d$ case, $t \cong s \cong \nu \cong 4/3$, in $3d$, the exponents are equal to $t \simeq 2.0$, $s \simeq 0.7$, and $\nu \simeq 0.88$ (Refs. 7 and 36)]. We set now the cube size l to be equal to

$$l = l_r = a(|\epsilon_m|/\epsilon_d)^{\nu/(t+s)}. \qquad (33)$$

Then, in the renormalized system, where each cube of the size l_r is considered as a single element, the dielectric constant of these new elements takes either value $\epsilon_m(l_r) = \epsilon_d^{t/(t+s)} |\epsilon_m|^{s/(t+s)} (\epsilon_m/|\epsilon_m|)$, for the element renormalized from the conducting cube, or $\epsilon_d(l_r) = \epsilon_d^{t/(t+s)} |\epsilon_m|^{s/(t+s)}$, for the element renormalized from the dielectric cube. The ratio of the dielectric constants of these new elements is equal to $\epsilon_m(l_r)/\epsilon_d(l_r) = \epsilon_m/|\epsilon_m| \cong -1 + i\kappa$, where the loss factor $\kappa = \epsilon_m''/|\epsilon_m| \ll 1$ is the same as in the original system. According to the basic ideas of the renormalization group transformation,[59,36] the concentration of conducting and dielectric elements does not change under the above transformation, provided that $p = p_c$. The field distribution in a two component system depends on the ratio of the dielectric permittivities of the components. Thus after the renormalization, the problem becomes equivalent to the considered above field distribution for the case $\epsilon_d = -\epsilon_m' = 1$. Taking into account that the electric field renormalizes as $E_0^{\star} = E_0(l_r/a)$, we obtain from Eq. (23) that the field peaks in the renormalized system are

$$E_m \simeq E_0 (a/\xi_A)^2 (l_r/a) \kappa^{-1} \simeq E_0 (a/\xi_A)^2 \left(\frac{|\epsilon_m|}{\epsilon_d} \right)^{\nu/(t+s)} \left(\frac{|\epsilon_m|}{\epsilon_m''} \right), \qquad (34)$$

where $\xi_A = \xi_A(p_c)$ is the localization length in the renormalized system. In the original system, each field maximum of the renormalized system locates in a dielectric gap in the "dielectric" cube of the l_r size or in-between two "conducting" cubes of the size l_r that are not necessarily connected to each other.[59] There is no a characteristic length in the original system that is smaller than l_r, except the microscopical length in the problem, which is a grain size a. Therefore, it is plausible to suggest that the width of a local-field peak in the original system is about a. Then the values of the field maxima E_m do not change when returning from the renormalized system to the original one. Therefore, Eq. (34) gives the values of the field maxima in the original system. Note

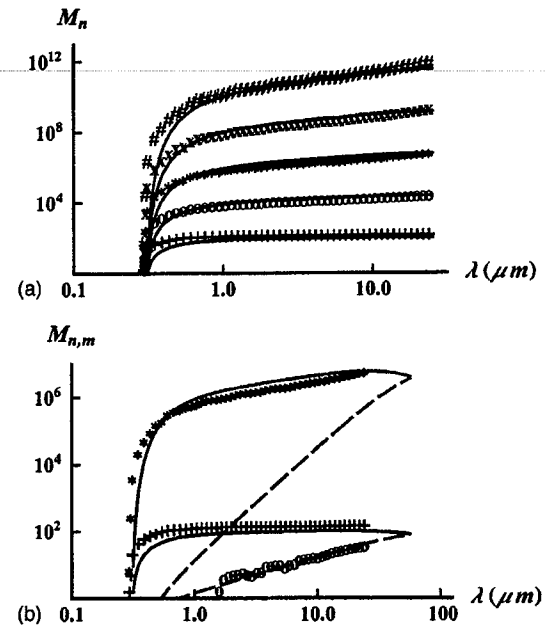

FIG. 3. High-order field moments of local electric field in semicontinuous silver films as a function of the wavelength λ at $p=p_c$. (a) Results of numerical calculations of $M_n \equiv M_{n,0}=\langle|E/E_0|^n\rangle$ for $n=2$, 3, 4, 5, and 6 are represented by +, 0, *, x, and #, respectively. The solid lines describe M_n found from the scaling formula (41). (b) $M_{4,0}=\langle|E/E_0|^4\rangle$ [scaling formula (41) - upper solid line, numerical simulations - *]; $M_{0,4}=\langle(E/E_0)^4\rangle$ [scaling formula (42) - upper dashed line]; $M_{2,0}=\langle|E/E_0|^2\rangle$ [scaling formula (41) - lower solid line, numerical simulations - +]; $M_{0,2}=\langle(E/E_0)^2\rangle$ [scaling formula (42) - lower dashed line, numerical simulations - 0]. In all presented analytical calculations we set $\xi_A=2a$ and $\rho=1$ in Eqs. (41) and (42).

that value E_m of the field maxima is different from previously obtained estimate (23) due to the renormalization of the applied field E_0.

Equation (34) gives the estimate for the local field extrema when the real part ϵ_m' of the metal dielectric constant becomes negative. For metals ϵ_m increases in absolute value with the wavelength, when the frequency ω is smaller than $\tilde{\omega}_p$ [see discussion below Eq. (1)]. Therefore, the field peaks $E_m(\omega)$ increase strongly with the wavelength (see, for example, Fig. 3 in our previous paper[10]). For a Drude metal it happens for the frequencies $\omega \lesssim \tilde{\omega}_p$, when the dielectric constant ϵ_m can be approximated as

$$\epsilon_m(\omega \lesssim \tilde{\omega}_p) \cong 2(\omega-\tilde{\omega}_p)\frac{\epsilon_b}{\tilde{\omega}_p}+i\frac{\epsilon_b\omega_\tau}{\tilde{\omega}_p}. \tag{35}$$

By substituting this expansion in Eq. (34), we obtain

$$E_m(\omega \lesssim \tilde{\omega}_p) \simeq E_0(a/\xi_A)^2\left(\frac{2\epsilon_b|\omega-\tilde{\omega}_p|}{\tilde{\omega}_p}\right)^{(\nu+t+s)/(t+s)}\frac{\tilde{\omega}_p}{\omega_\tau\epsilon_b\epsilon_d^{\nu/(t+s)}}. \tag{36}$$

Since losses in a typical metal are small, $\omega_\tau \ll \tilde{\omega}_p$, the field peak amplitudes first increase steeply and then saturate (see below) with the magnitude $E_m \simeq E_0(a/\xi_A)^2(\epsilon_b/\epsilon_d)^{\nu/(t+s)}(\tilde{\omega}_p/\omega_\tau) \sim E_0\tilde{\omega}_p/\omega_\tau$ at $\omega=0.5\tilde{\omega}_p$. Therefore, the intensity maxima I_m exceed the intensity of the incident wave I_0 by $I_m/I_0 \sim (\tilde{\omega}_p/\omega_\tau)^2 \gg 1$. For a silver-glass percolation composite we obtained $I_m/I_0 \sim 10^3$ (see also the field distribution in Figs. 1 and 2).

Now we consider the case of small frequencies $\omega \ll \omega_p$ when the dielectric constant ϵ_m for a Drude metal (see Eq. 1) takes the form

$$\epsilon_m(\omega \ll \omega_p) \cong -\left(\frac{\omega}{\omega_p}\right)^2\left(1-i\frac{\omega_\tau}{\omega}\right), \tag{37}$$

where we again assume that $\omega \gg \omega_\tau$. By substituting this expression in Eq. (34), we obtain

$$E_m(\omega \ll \omega_p) \simeq E_0\left(\frac{a}{\xi_A}\right)^2\left(\frac{\omega_p}{\sqrt{\epsilon_d}\omega}\right)^{2\nu/(t+s)}\left(\frac{\omega}{\omega_\tau}\right). \tag{38}$$

For the $2d$ case, the critical exponents are equal to $\nu \cong t \cong s \cong 4/3$ and Eq. (38) gives $E_m \sim (a/\xi_A)^2E_0\omega_p/(\sqrt{\epsilon_d}\omega_\tau) = (a/\xi_A)^2E_0\sqrt{\epsilon_b/\epsilon_d}(\tilde{\omega}_p/\omega_\tau)$, that coincides with the estimate obtained from Eq. (36) for $\omega=0.5\tilde{\omega}_p$. This means that the local-field peaks increase steeply when the real part of the metal dielectric constant ϵ_m becomes negative $\epsilon_m'<0$ and then remain almost the same in the wide frequency range $\tilde{\omega}_p<\omega<\omega_\tau$, for $2d$ composites.

For $3d$ percolation composites, the critical exponents are equal to $\nu \cong 0.88$, $t \cong 2.0$, $s \cong 0.7$.[7] To simplify estimations we put below $\nu \cong (t+s)/3$ for $d=3$. Then Eq. (38) takes the following form $E_m \sim E_0(\epsilon_b/\epsilon_d)^{1/3}\tilde{\omega}_p^{2/3}\omega^{1/3}/\omega_\tau$, that is the local-field peaks increase up to $E_m/E_0 \sim \tilde{\omega}_p/\omega_\tau$ when ϵ_m' becomes negative and then the peaks decrease as $E_m/E_0 \sim (\tilde{\omega}_p/\omega_\tau)(\omega/\tilde{\omega}_p)^{1/3}$, with further decrease of frequency. For silver composites, we estimate that the maximum value of the peaks is achieved at $\omega \cong 0.5\tilde{\omega}_p$ that corresponds to $\lambda \cong 0.6$ μm.

Since we know the peak amplitudes for the local electric field we can estimate the moments $M_{n,m}$ of the local field. To obtain $M_{n,m}$, we consider first spatial distribution of the field maxima for $|\epsilon_m| \gg \epsilon_d$. The average distance between the field maxima in the renormalized system is equal to ξ_e^* given by Eq. (24). Then the average distance ξ_e between the field maxima in the original system (provided that $\rho \sim 1$) is equal to

$$\xi_e \cong (l_r/a)\xi_e^* \sim a\left(\frac{|\epsilon_m|}{\epsilon_d}\right)^{\nu/(t+s)}\left(\frac{|\epsilon_m|}{\epsilon_m''}\right)^{1/d}. \tag{39}$$

In the original system, each field maximum of the renormalized system splits into $n(l_r)$ peaks of the E_m amplitude located along a dielectric gap in the "dielectric" cube of the l_r size. The gap "area" scales as the capacitance of the dielectric cube, so does the number of peaks

$$n(l_r) \propto (l_r/a)^{d-2+s/\nu}. \tag{40}$$

There are, on average, $(\xi_A/a)^d$ excited clusters. Thus, we obtain the following estimate for the local-field moments

$$M_{n,m}\sim(\xi_A/a)^d\left(\frac{E_m}{E_0}\right)^{n+m}\frac{n(l_r)}{(\xi_e/a)^d}$$
$$\sim\rho(\xi_A/a)^{d-2(n+m)}\left(\frac{l_r/a}{\kappa}\right)^{n+m-1}(l_r/a)^{s/\nu-1}$$
$$\sim\rho(\xi_A/a)^{d-2(n+m)}\left[\left(\frac{|\epsilon_m|}{\epsilon_d}\right)^{\nu/(t+s)}\right]^{n+m-2+s/\nu}$$
$$\times\left(\frac{|\epsilon_m|}{\epsilon_m''}\right)^{n+m-1} \tag{41}$$

that holds for $n+m>1$ and $n>0$. Since $|\epsilon_m|\gg\epsilon_d$ and the ratio $|\epsilon_m|/\epsilon_m''\gg1$ the moments of the local field are very large, $M_{n,m}\gg1$, in the visible and infrared spectral ranges. Note that the first moment $M_{0,1}\sim1$ that corresponds to the equation $\langle\mathbf{E}(\mathbf{r})\rangle=\mathbf{E}_0$. We stress again that the localization length ξ_A in Eq. (41) corresponds to the renormalized system with $\epsilon_d=-\epsilon_m'=1$. The localization length in the original system, i.e., a typical size of the eigenfunction is estimated as $(l_r/a)\xi_A\gg a$. In other words the eigenstates become macroscopically large in the limit of large contrast $|\epsilon_m|/\epsilon_d\gg1$ and consist of sharp peaks separated in space by distance much larger than a. The eigenstates of HK $\hat{\mathrm{H}}$ cover the volume $(\xi_A l_r/a)^d\sim(\xi_A\omega_p/\omega)^d\gg a^d$ for two-dimensional Drude metal composites and $\omega\ll\omega_p$.

We consider now the moments $M_{n,m}$ for $n=0$ that correspond to the volume average of the mth power of the complex amplitude $E(\mathbf{r})$, namely, $M_{0,m}=\langle E^m(\mathbf{r})\rangle/E_0^m$. In the renormalized system, where $|\epsilon_m(l_r)|=|\epsilon_d(l_r)|$ and $\epsilon_m(l_r)/\epsilon_d(l_r)\cong-1+i\kappa$, the field distribution coincides with the field distribution in the system with $\epsilon_d\simeq-\epsilon_m'\sim1$. In the system with $\epsilon_d\simeq-\epsilon_m'\sim1$ the field peaks $E_m^\star$ are different in phase and because of the destructive interference, the moment $M_{0,m}^\star\sim O(1)$ [as it follows from Eq. (31)]. In transition to the original system the peaks increase by the factor l_r/a, leading to the corresponding increase of the moment $M_{0,m}$. We suppose that within a single "dielectric" cube the field peaks are in phase, i.e., the field maxima form chains of aligned peaks that are stretched out in a dielectric cube. This assumption is confirmed by results of numerical simulation shown in Fig. 1, where the field maxima with different signs are concentrated in different places of a percolation composite. Then we obtain the following equation for the moment:

$$M_{0,m}\sim M_{0,m}^\star(l_r/a)^m\frac{n(l_r)}{(\xi_e/a)^d}\sim\kappa(l_r/a)^{m-2+s/\nu}$$
$$\sim\left(\frac{\epsilon_m''}{|\epsilon_m|}\right)\left(\frac{|\epsilon_m|}{\epsilon_d}\right)^{(m-2+s/\nu)\nu/(t+s)}, \tag{42}$$

which holds when $M_{0,m}$ given by this equation is larger than one.

Using the critical exponents for $2d$ percolating composites, $t\cong s\cong\nu\cong4/3$,[7] we can simplify Eqs. (41) and (42) as follows

$$M_{n,m}\sim\rho\left[\frac{|\epsilon_m|^{3/2}}{(\xi_A/a)^2\sqrt{\epsilon_d}\epsilon_m''}\right]^{n+m-1}\quad(d=2), \tag{43}$$

for $n+m>1$ and $n>0$, and

$$M_{0,m}\sim\frac{\epsilon_m''|\epsilon_m|^{(m-3)/2}}{\epsilon_d^{(m-1)/2}}\quad(d=2), \tag{44}$$

for $m>1$, $n=0$ and $(|\epsilon_m|/\epsilon_d)^{(m-1)/2}>|\epsilon_m|/\epsilon_m''$ [the last inequality corresponds to the condition that the moment given by Eq. (44) is larger than one]. The moments $M_{n,m}(n\neq0)$ are strongly enhanced in $2d$ Drude metal-dielectric composites. The moments reach the maximum value

$$M_{n,m}\sim\rho\left[\frac{\omega_p}{\omega_\tau\sqrt{\epsilon_d}(\xi_A/a)^2}\right]^{n+m-1}\quad(d=2), \tag{45}$$

when frequency ω decreases so that the condition $\omega\ll\omega_p$ is fulfilled. The spatial moments of the local electric in a $2d$ percolation composite are independent of frequency, for $\omega\ll\omega_p$. For metals it typically takes place in the red and infrared spectral ranges. For a silver semicontinuous film on a glass substrate, the moment $M_{n,m}$ can be estimated as $M_{n,m}\sim[(a/\xi_A)^2 3\times10^2]^{n+m-1}$, for $\omega\ll\omega_p$.

It follows from Eq. (41) that for $3d$ metal-dielectric percolation composites, where the dielectric constant of metal component can be estimated by the Drude formula (1), the moments $M_{n,m}$ $(n\neq0)$ achieve the maximum value at frequency $\omega_{\max}\approx0.5\tilde{\omega}_p$. To estimate the maximum value, we note that the following relations $\nu/(t+s)\approx1/3$, $s\approx\nu$ are valid for the $3d$ case, where $t\cong2.0$, $s\cong0.7$ and $\nu\cong0.88$.[7] Then the maximum value of the moments is estimated as

$$M_{n,m}(\omega=\omega_{\max})$$
$$\sim\rho(\xi_A/a)[(a/\xi_A)^2(\epsilon_b/\epsilon_d)^{1/3}\tilde{\omega}_p/\omega_\tau]^{n+m-1}\quad(d=3). \tag{46}$$

For small frequencies $\omega\ll\omega_p$, the moments of the local field decrease with the wavelength as

$$M_{n,m}(\omega\ll\omega_p)\sim\rho(\xi_A/a)\left[\frac{(a/\xi_A)^2\omega_p^{2/3}\omega^{1/3}}{\epsilon_d^{1/3}\omega_\tau}\right]^{n+m-1}\quad(d=3). \tag{47}$$

In Fig. 3, we compare results of numerical and theoretical calculations for the field moments in $2d$ silver semicontinuous films on glass. We see that there is excellent agreement between the scaling theory [formulas (43) and (44)] and numerical simulations. To fit the data we used $\xi_A\approx2a$. [Results of numerical simulations for $M_{0,4}$ are not shown in Fig. 3 since it was not possible to achieve reliable results in the simulations because of large fluctuations in values of this moment.] The small value of ξ_A indicates strong localization of surface plasmons in percolation composites, at least for the $2d$ case. As seen in Fig. 3(b) the spectral dependence of enhancement $M_{n,m}$ differs strongly for processes with $(n\neq0)$ and without $(n=0)$ subtraction of photons.

As discussed above, nonlinear optical processes, in general, are phase dependent and proportional to a factor $|E|^nE^m$, i.e., they depend on the phase through the term E^m and their enhancement is estimated as $M_{n,m}=\langle|E/E^{(0)}|^n(E/E^{(0)})^m\rangle$. According to the above consideration, $M_{n,m}\sim M_{n+m,0}$, for $n\geq1$. For example, enhancement

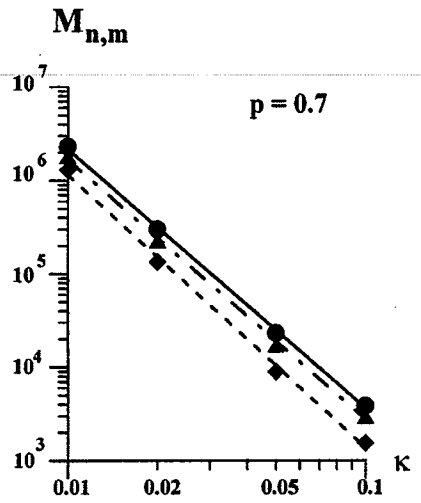

FIG. 4. Fourth-order field moments $M_{m,n}$ $(m+n=4)$ of the local electric field in $2d$ metal-dielectric composite with $\epsilon_d=1$ and metal permittivity $\epsilon_m=-100(1-i\kappa)$, as functions of κ: $M_{4,0}$–●, $M_{3,1}$–▲, $M_{2,2}$–■.

of the Kerr-type nonlinearity $G_K=M_{2,2}\sim G_{RS}\simeq M_{4,0}$; (see also next section). For nearly degenerate four-wave mixing (FWM), the enhancement is given by $G_{FWM}\sim|G_K|^2\sim|M_{2,2}|^2$ and can reach giant values up to $\sim 10^{12}$.

Above, for the sake of simplicity, we assumed that $p=p_c$ when considering the case of $\epsilon_m'\ll 0$. Now we estimate the concentration range $\Delta p=p-p_c$, where the above estimates for the local field moments are valid.[28,29] We note that the above expressions for the local field and average field moments $M_{n,m}$ hold in almost all concentration range given by Eq. (25) when $\epsilon_m\simeq-\epsilon_d$. The metal concentration range Δp, where the local electric field is strongly enhanced, shrinks, however, when $\epsilon_m'\ll 0$. The above speculations are based on the finite-size scaling arguments, which hold provided the scale l_r of the renormalized cubes is smaller than the percolation correlation length $\xi\cong a(|p-p_c|/p_c)^{-\nu}$. At the percolation threshold, where the correlation length ξ diverges, our estimates are valid in a wide frequency range $\omega_\tau<\omega<\tilde{\omega}_p$, which includes the visible, infrared, and far-infrared spectral ranges for a typical metal. For any particular frequency from this interval, we estimate the concentration range Δp , where the giant field fluctuations occur, by equating the values of l_r and ξ, which results in the inequality $|\Delta p|\leqslant(\epsilon_d/|\epsilon_m|)^{1/(t+s)}$.

In Fig. 4, we show the moments $M_{4,0}$, $M_{3,1}$, and $M_{2,2}$ as a function of κ for $2d$ percolating system with $\epsilon_m=100(-1+i\kappa)$, $\epsilon_d=1$ and metal concentration $p=0.7>p_c=0.5$. All the moments are close in magnitude and increase with decreasing losses κ according to a power-law dependence with the same exponent, as it is predicted by Eq. (43).

III. GIANT ENHANCEMENTS OF OPTICAL NONLINEARITIES AND RAMAN SCATTERING IN PERCOLATION COMPOSITES

In this section, we consider enhancements for nth harmonic generation, Raman and hyper-Raman scattering, and Kerr nonlinearity in metal-dielectric composites. To develop our previous considerations,[10] we obtain here scaling formulas for enhancement factors for different nonlinear optical processes, including those that depend on the field phase. The enhancement is expressed in terms of the high-order field moments considered above. We again assume that the light wavelength λ is larger than any intrinsic spatial scale in the film, including the skin depth, $\lambda\gg a\sqrt{|\epsilon_m|}$. We do not consider here the effects of light propagation and suppose that $\mathbf{E}_0$ is the macroscopic, average electric field acting in the system. The field $\mathbf{E}_0$ changes on the spatial scale of the order of λ, which is much larger than the scale of the microscopic averaging. For simplicity, we also assume that $\mathbf{E}_0$ is linearly polarized so that it can be chosen real.

A. High harmonic generation

We consider here enhanced nth harmonic generation (nHG) at frequency $n\omega$ when a percolation metal-dielectric composite is irradiated by a light beam at frequency ω. For estimations, we assume, as above, that metal grains are characterized by the Drude dielectric function given by Eq. (1). As shown in previous sections, Anderson localization of surface plasmon excitations results in giant scale-invariant field fluctuations of the local electric field. This makes the considered here high harmonic generation different from the well-known phenomena of harmonic generation from smooth[60–64] and rough[65–69] surfaces.

We assume that the material components forming a composite possess nonlinear conductivity $\sigma^{(n)}$ that results in nHG; $\sigma^{(n)}$ can also be due to adsorbed molecules in the composite. As shown in Sec. II, the local field concentrates mainly in dielectric gaps between metal clusters. Therefore, largest enhancement of nonlinear effects is achieved when either nonlinear adsorbed molecules are located in the dielectric gaps or the dielectric itself possesses the nonlinearity.

The local electric field $\mathbf{E}_\omega(\mathbf{r})$ induced in a composite by the external field $\mathbf{E}_{\omega,0}$ generates the $n\omega$ current $\sigma^{(n)}\mathbf{E}_\omega(\mathbf{r})E_\omega^{n-1}(\mathbf{r})$ in the system. This expression, strictly speaking, holds only for the scalar nonlinear conductivity and odd n (i.e., $n=2k+1$), when $E^{n-1}=(\mathbf{E}\cdot\mathbf{E})^k$. However, for estimates, the formula can be used in the general case, for arbitrary n. The nonlinear current interacts with the system and generates the "seed" $n\omega$ electric field, with the amplitude $\mathbf{E}_{n\omega}^{(s)}=\sigma^{(n)}E_\omega^{n-1}\mathbf{E}_\omega/\sigma^{(1)}$, where $\sigma^{(1)}$ is the *linear* conductivity at frequency $n\omega$. The electric field $\mathbf{E}_{n\omega}^{(s)}$ can be thought of as an inhomogeneous external field exciting the composite at $n\omega$ frequency. The nHG current $\mathbf{j}_{n\omega}$ induced in the film by the "seed" field $\mathbf{E}_{n\omega}^{(s)}$ can be found in terms of the nonlocal conductivity tensor $\hat{\Sigma}(\mathbf{r},\mathbf{r}')$ that relates the applied (external) field at point $\mathbf{r}'$ to the current at point $\mathbf{r}$, $j_{n\omega,\beta}(\mathbf{r})=\int\Sigma_{n\omega,\beta\alpha}(\mathbf{r},\mathbf{r}')E_{n\omega,\alpha}^{(s)}(\mathbf{r}')d\mathbf{r}'$, where $\Sigma_{n\omega,\beta\alpha}$ is the conductivity tensor at frequency $n\omega$ and the integration is over the entire film area.[10,30] The Greek indices take values $\{x,y\}$ for $d=2$ and $\{x,y,z\}$ for $d=3$. The summation over repeated indices is implied. It is the current $\mathbf{j}_{n\omega}$ that eventually generates the nonlinear scattered field at the frequency $n\omega$. Figure 1 shows the normalized real part of the 3ω local field $g_3'=\mathrm{Re}[E^2(\mathbf{r})E_x(\mathbf{r})]/|E^{(0)}|^3$ in a $2d$ silver-on-glass film. As seen in Fig. 1, the fluctuating 3ω fields form a set of

sharp peaks, looking up and down, and having the magnitudes $\sim 10^3 \div 10^6$. Such huge fluctuations of the local fields are anticipated to strongly enhance the 3ω and higher harmonic generation.

For simplicity, we assume that the metal and dielectric components of a composite have the same nonlinear conductivity $\sigma^{(n)}$ (e.g., resulting from adsorbed molecules uniformly distributed in the composite). We are interested in enhancement of the $n\omega$ harmonic generation due to the giant local field fluctuations. Therefore, we compare the $n\omega$ signal from the system with and without metal grains. It is shown in our previous paper[10] that enhancement of the nth harmonic generation is given by the following formula

$$G_{nHG} \sim \left| \frac{\langle \sigma_{n\omega}(\mathbf{r})[\mathbf{E}_{n\omega}(\mathbf{r})\cdot\mathbf{E}_{\omega}(\mathbf{r})]E_{\omega}^{n-1}(\mathbf{r})\rangle}{\sigma_d E_{\omega,0}^{n+1}} \right|^2 = \left| \frac{\langle \epsilon_{n\omega}(\mathbf{r})[\mathbf{E}_{n\omega}(\mathbf{r})\cdot\mathbf{E}_{\omega}(\mathbf{r})]E_{\omega}^{n-1}(\mathbf{r})\rangle}{\epsilon_d E_{\omega,0}^{n+1}} \right|^2, \quad (48)$$

where $\mathbf{E}_{n\omega}(\mathbf{r})$ is the local electric field exited in the system by *uniform* probe field $\mathbf{E}_{n\omega,0}$ that has the same amplitude and direction as external field $E_{\omega,0}$ but oscillates with the frequency $n\omega$; $\sigma_{n\omega}(\mathbf{r})$, σ_d and $\epsilon_{n\omega}(\mathbf{r})$, ϵ_d are the linear conductivities and dielectric functions of the composite with and without metal grains, respectively. The enhancement G_{nHG} does not depend on the amplitude of the external field and is essentially an intrinsic property of the system. The local fields in Eq. (48), resulting in enhancement of nth harmonic generation, experience giant fluctuations in the spectral band of the plasmon resonances, i.e., for $\omega_\tau < \omega, n\omega < \tilde{\omega}_p$, as shown in Sec. II. This includes the optical, infrared, and far-infrared spectral ranges, where the huge enhancement of nth harmonic generation can be observed in percolation composites. When frequency ω of the incident wave is large enough so that the nth harmonic $n\omega$ is out of the spectral range of the plasmon resonances, i.e., $n\omega > \tilde{\omega}_p$, we can neglect the fluctuations of the $n\omega$ field in Eq. (48) and this equation simplifies to

$$G_{nHG,0} \sim \left| \frac{\langle \sigma_{n\omega}(\mathbf{r})\mathbf{E}_{\omega}(\mathbf{r})E_{\omega}^{n-1}(\mathbf{r})\rangle}{\sigma_d E_{\omega,0}^{n}} \right|^2 = \left| \frac{\langle \epsilon_{n\omega}(\mathbf{r})\mathbf{E}_{\omega}(\mathbf{r})E_{\omega}^{n-1}(\mathbf{r})\rangle}{\epsilon_d E_{\omega,0}^{n}} \right|^2. \quad (49)$$

As shown in Sec. II, fields with different frequencies ω fluctuate in space with different spatial scales $\xi_e(\omega)$. Therefore we can use decoupling in Eq. (48) to obtain the following estimate

$$G_{nHG} \sim \left| \frac{\langle \epsilon_{n\omega}(\mathbf{r})\mathbf{E}_{n\omega}(\mathbf{r})\rangle \cdot \langle \mathbf{E}_{\omega}(\mathbf{r})E_{\omega}^{n-1}(\mathbf{r})\rangle}{\epsilon_d E_{\omega,0}^{n+1}} \right|^2 \sim \frac{|\langle \epsilon_{n\omega}(\mathbf{r})\mathbf{E}_{n\omega}(\mathbf{r})\rangle|^2}{\epsilon_d^2 E_{n\omega,0}^2} \frac{|\langle \mathbf{E}_{\omega}(\mathbf{r})E_{\omega}^{n-1}(\mathbf{r})\rangle|^2}{E_{\omega,0}^{2n}} = \frac{|\epsilon_e(n\omega)|^2}{\epsilon_d^2} |M_{0,n}|^2, \quad (50)$$

where $\mathbf{E}_{n\omega}(\mathbf{r})$ is the local field exited in the system by the uniform field $\mathbf{E}_{n\omega,0}$ with frequency $n\omega$, $\epsilon_e(n\omega)$ is the effective dielectric constant of the composite at frequency $n\omega$, and the moment $M_{0,n}$ is determined by Eq. (26). Strictly speaking, this equation holds for $n\omega < \tilde{\omega}_p$, but we can use it in the whole frequency range since the metal dielectric constant $\epsilon_m(n\omega)$ is of the order of one for $n\omega > \tilde{\omega}_p$ and Eq. (50) gives the same result as Eq. (49) for $n\omega > \tilde{\omega}_p$. At the percolation threshold the effective conductivity is estimated as $\epsilon_e(n\omega) \sim \epsilon_d(\epsilon_m(n\omega)/\epsilon_d)^{s/(t+s)}$, where s and t are percolation critical exponents for the dielectric constant and conductivity, respectively.[7] Substituting this result together with Eq. (42) for the moment $M_{0,n}$ in Eq. (50), we obtain the following expression for the nth harmonic enhancement

$$G_{nHG} \sim \left[\frac{|\epsilon_m(n\omega)|}{\epsilon_d} \right]^{2s/(t+s)} \left[\frac{\epsilon_m''}{|\epsilon_m|} \right]^2 \left[\frac{|\epsilon_m(\omega)|}{\epsilon_d} \right]^{2(n-2+s/\nu)\nu/(t+s)}. \quad (51)$$

For a Drude metal and $n\omega \ll \omega_p$, we have $|\epsilon_m| \sim |\epsilon_m(n\omega)| \sim (\omega_p/\omega)^2$ and $\epsilon_m''/|\epsilon_m| \sim \omega_\tau/\omega$. For estimates, we can set $s/\nu \simeq 1$, which holds for $d=2$ and $d=3$ as well. Then Eq. (51) acquires the following form

$$G_{nHG} \sim \left(\frac{\omega_\tau}{\omega}\right)^2 \left(\frac{\omega_p}{\omega}\right)^{4n\nu/(t+s)}. \quad (52)$$

For $2d$ systems, where the critical exponents are equal to $s \simeq t \simeq \nu = 4/3$, Eq. (52) gives the simple formula for G_{nHG}

$$G_{nHG} \sim \left(\frac{\omega_\tau}{\omega}\right)^2 \left(\frac{\omega_p}{\omega}\right)^{2n}, \quad (d=2). \quad (53)$$

For $3d$ system, where the critical exponent $\nu \approx (t+s)/3$, Eq. (52) can be simplified as

$$G_{nHG} \sim \left(\frac{\omega_\tau}{\omega}\right)^2 \left(\frac{\omega_p}{\omega}\right)^{4n/3}, \quad (d=3). \quad (54)$$

We can estimate enhancement of second and third harmonics in silver-on-glass semicontinuous film as $G_{2HG} \sim 2 \times 10$ and $G_{3HG} \sim 2 \times 10^3$, for $\lambda = 1.5$ μm, and $G_{2HG} \sim 10^3$ and $G_{3HG} \sim 5 \times 10^5$, for $\lambda = 3.0$ μm. These estimates are in agreement with our numerical calculations.[10] In particular, the simulations indicate that $G_{2HG} \sim \omega^{-6}$ in the long-wavelength limit, which is exactly the result given by Eq. (53).

We note that the obtained formulas define enhancement for a coherent signal of harmonic generation propagating in the reflected or transmitted direction. As shown in Ref. 70, the coherent harmonic generation is accompanied by a diffusive broad-angle nonlinear scattering at frequency $n\omega$, with the integral enhancement exceeding the coherent signal by many orders of magnitude. This phenomenon dubbed in Ref. 70 as percolation enhanced nonlinear scattering (PENS) has been observed in experiments,[71] but was not explained at the time.

It follows from Eq. (53) that enhancement increases with n, so that $G_{n+1HG}/G_{nHG} = (\omega_p/\omega)^2$ is much larger than one.

It is interesting to note that the fact that enhancement strongly increases with the order of the optical nonlinearity can result in unusual situation when, for example, second-harmonic generation (SHG) is dominated by higher-order nonlinearity $\chi^{(4)}(-2\omega;\omega,\omega,-\omega,\omega)$, rather than being due to $\chi^{(2)}(-2\omega;\omega,\omega)$. This is because $M_{2,2}$, which is responsible for enhancement of the above $\chi^{(4)}(-2\omega;\omega,\omega,-\omega,\omega)$, at some wavelengths ($\sim 1$ μm) can exceed $M_{0,2}$, by many orders of magnitude. For example, in semicontinuous metal films the ratio of the moments $M_{2,2}$ and $M_{0,2}$ at the percolation can be estimated from Eqs. (43) and (44) as $M_{2,2}/M_{0,2}\sim(a/\xi_A)^6|\epsilon_m|^5/\epsilon_d\epsilon_m''^4$, where we set the density of states $\rho\simeq 1$. Substituting here $\epsilon_d=2.2$, which corresponds to the glass substrate, and parameters for the silver dielectric constant we obtain the estimate $M_{2,2}/M_{0,2}\sim(a/\xi_A)^6 10^7$, for $\omega\ll\omega_p$. Another possible situation is when hyper-Raman scattering (considered below) is as efficient as "conventional" Raman scattering. Also, we note that when higher-order nonlinearities compete with lower-order nonlinearities, a bistable behavior can be obtained, which can be used in various applications in optoelectronics.

B. Raman and hyper-Raman scattering

Surface-enhanced Raman scattering (SERS) from various nanostructured random media (rough films, colloidal aggregates, etc.), is one of most intriguing optical effects discovered in the last two decades.[72–74] Recent studies indicate that SERS is especially large in strongly disordered media, such as fractal small-particle composites and self-affine thin films, where the local-field fluctuations are especially large because of strong spatial localization of optical modes in different random parts of the object.[9] Because of the sp localization in percolation composites, SERS also experiences giant enhancement in these media.[30]

In most studies, the average (integrated) SERS was considered. Recently, it was shown that the local enhancements in the hot spots can exceed the average enhancement by many orders of magnitude making possible SERS from single molecules.[31,73,74]

It was shown in our previous papers[10,31] that the SERS enhancement is given by $G_{RS}\sim M_{4,0}=\langle|E(\mathbf{r})/E_0|^4\rangle$. Using Eq. (41), we obtain

$$G_{RS}\sim\rho(p)[\xi_A(p)/a]^{d-8}\left(\frac{|\epsilon_m|}{\epsilon_d}\right)^{(2\nu+s)/(t+s)}\left(\frac{|\epsilon_m|}{\epsilon_m''}\right)^3, \tag{55}$$

where we indicated explicitly dependence of the density of states $\rho(p)$ and localization length $\xi_A(p)$ on the concentration p of metal grains. Thus, the obtained Raman enhancement G_{RS} depends strongly on localization length ξ_A. When the states are delocalized $\xi_A\to\infty$ and G_{RS} vanishes very rapidly.

Now we consider frequency and concentration dependence of Raman scattering predicted by Eq. (55). For $2d$ composites and frequency $\omega\ll\omega_p$ Eq. (55) results in the enhancement $G_{RS}\sim\rho(p)[a/\xi_A(p)]^6(\omega_p/\omega_\tau)^3/\epsilon_d^{3/2}$, which is independent of frequency. For silver-on-glass percolation films we set $\xi_A\approx 2a$ according to our computer simulations [see Figs. (1) and (2)] and density of state $\rho(p_c)\sim 1$ [see discussion after Eq. (12)]. Thus, we obtain the SERS enhancement $G_{RS}\sim 10^6$ silver semicontinuous films at the percolation threshold. For $3d$ composite at $\omega\ll\omega_p$, SERS decreases with decreasing frequency as $G_{RS}\sim\rho(p)\times(\xi_A/a)^{-5}\omega_p^2\omega/\omega_\tau^3\sim 10^6\omega/\omega_p$, where we used for estimates $\xi_A\approx 2a$, $\rho\sim 1,\nu\approx s\approx(t+s)/3$ and substitute the data $\omega_p=9.1$ eV and $\omega_\tau=0.021$ eV for silver.[57]

The localization radius ξ_A of the eigenstates Ψ_n with eigenvalues $\Lambda\approx 0$ decreases when we shift from $p=p_c$ toward $p=0$ or $p=1$ since the eigenvalue $\Lambda=0$ shifts from the center of the Λ distribution to its tails, where localization of the eigenstates is stronger. Therefore, according to Eq. (55), Raman scattering has a *minimum* at the percolation threshold. As a result, the double maximum dependence $G_{RS}(p)$ takes place as was observed in experiments and numerical calculations,[31] with one maximum below the percolation threshold p_c and another above the p_c.

The intensity of the local Stokes sources $I_{RS}(\mathbf{r})\propto|E(\mathbf{r})|^4$ (provided the Stokes shift of frequency is small) follows the local-field distribution. In the peaks (hot spots), Eq. (34) gives

$$I_{RS,\max}\propto|E(\mathbf{r})|^4\sim E_0^4(a/\xi_A)^8\left(\frac{|\epsilon_m|}{\epsilon_d}\right)^{4\nu/(t+s)}\left(\frac{|\epsilon_m|}{\epsilon_m''}\right)^4. \tag{56}$$

For a $2d$ Drude metal at $p=p_c$ and $\omega\ll\omega_p$, we estimate $I_{RS,\max}\propto|E(\mathbf{r})|^4/E_0^4\sim(\xi_A/a)^{-8}(\omega_p/\omega_\tau)^4\gg 1$. If the density of Raman-active molecules is small enough, then each peak of the local field can be due to Raman scattering from a *single* molecule.

Consider now hyper-Raman scattering when n photons of frequency ω are converted in one hyper-Stokes photon of the frequency $\omega_{hRS}=n\omega-\Omega$, where Ω is the Stokes frequency shift corresponding to the frequency of molecule oscillations (electronic or vibrational). Following the approach developed in Ref. 29 we obtain the following result for surface-enhanced hyper-Raman scattering (SEHRS)

$$G_{hRS}=\frac{\langle|\sigma_{hRS}(\mathbf{r})|^2|\mathbf{E}_{hRS}(\mathbf{r})|^2|E(\mathbf{r})|^{2n}\rangle}{|\sigma_d|^2|E_{0,hRS}|^2|E_0|^{2n}}=\frac{\langle|\epsilon_{hRS}(\mathbf{r})|^2|\mathbf{E}_{hRS}(\mathbf{r})|^2|E(\mathbf{r})|^{2n}\rangle}{|\epsilon_d|^2|E_{0,hRS}|^2|E_0|^{2n}}, \tag{57}$$

where $\mathbf{E}_{hRS}(\mathbf{r})$ is the local-field excited in the system by the uniform probe field $\mathbf{E}_{0,hRS}$ oscillating with ω_{hRS}; $\sigma_{hRS}(\mathbf{r})$ and $\epsilon_{hRS}(\mathbf{r})$ are the local conductivity and dielectric constant at the frequency ω_{hRS}. At $n=1$ formula (57) describes the conventional SERS.

To estimate G_{hRS} we take into account that the spatial scales for the local field fluctuations, ξ_e, at the fundamental frequency ω and hyper-Stokes frequency ω_{hRS} are significantly different. Therefore, we can decouple the average in Eq. (57) and approximate it by

$$\begin{aligned}&\langle|\epsilon_{hRS}(\mathbf{r})|^2|\mathbf{E}_{hRS}(\mathbf{r})|^2|E(\mathbf{r})|^{2n}\rangle\\&\quad\sim\langle|\epsilon_{hRS}(\mathbf{r})\mathbf{E}_{hRS}(\mathbf{r})|^2\rangle\langle|E(\mathbf{r})|^{2n}\rangle\\&\quad=\langle|\epsilon_{hRS}(\mathbf{r})\mathbf{E}_{hRS}(\mathbf{r})|^2\rangle M_{2n,0}|E_0|^{2n}.\end{aligned}$$

It follows from the scaling analysis of the current-current correlation function fulfilled in Refs. 57 and 58 that the second moment of the current $\langle|\epsilon_{hRS}(\mathbf{r})\mathbf{E}_{hRS}(\mathbf{r})|^2\rangle$ is estimated as $\epsilon_d^2[\epsilon_m(\omega_{hRS})/\epsilon_d]^{(t+2s)/(t+s)}M_{2,0}^{\star}|E_{0,hRS}|^2$, where the moment $M_{2,0}^{\star}$ is given by Eq. (32). By substituting these results in Eq. (57), we obtain

$$G_{hRS}\sim[|\epsilon_m(\omega_{hRS})|/\epsilon_d]^{(t+2s)/(t+s)}M_{2,0}^{\star}M_{2n,0}, \quad (58)$$

where the moment $M_{2,0}^{\star}$ is taken at frequency ω_{hRS}. Now we use the expressions for moments $M_{2,0}^{\star}$ and $M_{2n,0}$ given by Eqs. (32) and (41) and take into account that for $p\simeq p_c$ the density of states in Eq. (32) is about unity $\rho\sim 1$. Thus, we obtain the following formula for enhancement of hyper-Raman scattering

$$G_{hRS}\sim(\xi_A/a)^{2d-4(1+n)}\left[\frac{|\epsilon_m(\omega_{hRS})}{\epsilon_d}\right]^{(t+3s)/(t+s)}\left[\frac{|\epsilon_m(\omega_{hRS})|}{\epsilon_m''(\omega_{hRS})}\right]\times\left[\frac{|\epsilon_m(\omega)|}{\epsilon_d}\right]^{[2\nu(n-1)+s]/(t+s)}\left[\frac{|\epsilon_m(\omega)|}{\epsilon_m''(\omega)}\right]^{2n-1}, \quad (59)$$

where $n\geq 2$. For a Drude metal and frequencies $\omega\ll\tilde{\omega}_p$, $\omega_{hRS}\ll\tilde{\omega}_p$ the metal dielectric constant can be approximated as $|\epsilon_m(\omega_{hRS})|\sim|\epsilon_m(\omega)|\sim(\omega_p/\omega)^2$, $\epsilon_m''(\omega)/|\epsilon_m(\omega)|\sim\omega_\tau/\omega$ and Eq. (59) acquires the form

$$G_{hRS}\sim(\xi_A/a)^{2d-4(1+n)}\left(\frac{\omega_p}{\omega}\right)^{2[2\nu(n-1)+4s+t]/(t+s)}\left[\frac{\omega}{\omega_\tau}\right]^{2n}, \quad (60)$$

which holds in the vicinity to the percolation threshold. For $2d$ composites where the critical exponents are $t=s=\nu=4/3$ Eq. (59) simplifies to

$$G_{hRS}\sim(a/\xi_A)^{4n}\left(\frac{\omega_p}{\omega}\right)^{2(n+1)}\left(\frac{\omega_p}{\omega_\tau}\right)^{2n}, \quad (61)$$

which for $n=2$ in silver semicontinuous films is estimated as $G_{hRS}\sim 10^{14}(a/\xi_A)^8\lambda^2$, where the wavelength λ is given in microns. As above for Raman scattering, the local enhancement in the hot spots can be much larger than the average one.

C. Kerr-type third-order optical nonlinearity

For the Kerr-type nonlinearity the displacement current $\mathbf{D}$ in the simplest case can be written as[17]

$$\mathbf{D}=[\epsilon_e+\epsilon_e^{(3)}|\mathbf{E}_0|^2]\mathbf{E}_0, \quad (62)$$

where ϵ_e and $\epsilon_e^{(3)}$ are the effective linear and nonlinear dielectric constants. The nonlinear term is responsible, in particular, for the nonlinear refraction and nonlinear absorption.[17]

As shown, for example, in Ref. 10, the effective nonlinear dielectric constant $\epsilon_e^{(3)}$ in a random composite is given by

$$\epsilon_e^{(3)}=\frac{\langle\epsilon^{(3)}(\mathbf{r})E^2(\mathbf{r})|\mathbf{E}(\mathbf{r})|^2\rangle}{E_0^2|E_0|^2}, \quad (63)$$

where $\epsilon^{(3)}(\mathbf{r})$ is the local nonlinear dielectric constant of the composite. The local "Kerr field" $g_K=E^2(\mathbf{r})|\mathbf{E}(\mathbf{r})|^2/|E_0|^4$

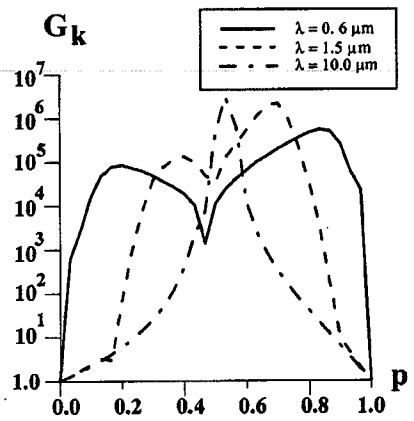

FIG. 5. Average enhancement of the Kerr optical nonlinearity $G_K=M_{2,2}$ in silver semicontinuous films as a function of the metal concentration p for three different wavelengths. The nonlinear Kerr permittivity $\epsilon^{(3)}$ is the same for metal and dielectric components.

in silver semicontinuous films is shown in Fig. 2. We are interested here in the average enhancement G_K (given by the integral of g_K over the system volume) of the Kerr nonlinearity $\epsilon_e^{(3)}$ due to fluctuations of the local fields in metal-dielectric composites. When the local field fluctuations are negligible, the effective nonlinear dielectric constant $\epsilon_e^{(3)}\sim\langle\epsilon^{(3)}(\mathbf{r})\rangle$.

We consider first the case when $\epsilon^{(3)}(\mathbf{r})$ in the dielectric component is of the same order of magnitude or larger than in the metal component. (The opposite case of almost linear dielectric $|\epsilon_d^{(3)}|\ll|\epsilon_m^{(3)}|$ will be considered below). Then the Kerr enhancement G_K is estimated as

$$G_K\sim\epsilon_e^{(3)}/\langle\epsilon^{(3)}(\mathbf{r})\rangle\sim M_{2,2}\sim\rho(\xi_A/a)^{d-8}\left(\frac{|\epsilon_m|}{\epsilon_d}\right)^{(2\nu+s)/(t+s)}\left(\frac{|\epsilon_m|}{\epsilon_m''}\right)^3, \quad (64)$$

where we used Eq. (41) for the moment $M_{2,2}$ of the local field. This expression for G_K coincides with Eq. (55) for the enhancement of Raman scattering. For $\omega\ll\omega_p$ the Kerr enhancement for $2d$ composites (semicontinuous metal films) is estimated as $G_K\sim\rho(\xi_A/a)^{d-8}(\omega_p/\omega_\tau)^3$ where we use the Drude formula (1) for the metal dielectric constant ϵ_m. For silver-on-glass semicontinuous films $\xi_A/a\approx 2$ and $\rho\approx 1$, we obtain $G_K\sim 10^6$.

In Fig. 5 we show results of numerical simulations for G_K as a function of the metal filling factor p, for $d=2$. The plot has a two-peak structure, as in the case of Raman scattering. However, in contrast to G_{RS}, the dip at $p=p_c$ is much stronger and at $p=p_c$ is proportional (as simulations show) to the loss factor κ. This implies that at $p=p_c$, the enhancement is actually given by $G_K\sim\kappa M_{2,2}$, where $M_{2,2}$ was found above. This result might be a consequence of the special symmetry of a self-dual system at $p=p_c$. Formally, it could happen if the leading term in the power expansion of $M_{2,2}$ over $1/\kappa$ cancels out because of the symmetry [see the discussion following Eq. (31)]. When this symmetry is somehow broken, e.g., by slightly moving away from the point $p=p_c$, the enhancement G_K increases and becomes $G_K\sim M_{2,2}\sim G_{RS}\sim M_{4,0}$, as seen in Fig. 4. The fact that the minimum at p

$=p_c$ is much less for SERS than for the Kerr process is probably related to the fact that the latter is a phase sensitive effect.

As shown in Sec. II, the local field maxima are concentrated in the dielectric gaps when $|\epsilon_m| \gg \epsilon_d$. Therefore, the enhancement estimate in Eq. (64) is valid when the Kerr nonlinearity is located in these gaps (it can be due to the dielectric itself or due to adsorbed molecules).

Consider now the case when the Kerr nonlinearity is due to metal grains as in recent experiment.[11] Provided that $\epsilon'_m \cong -\epsilon_d$, the local electric field are equally distributed in metal and dielectric components. Therefore, the Kerr enhancement is still given by Eq. (64) where one should set $|\epsilon_m|/\epsilon_d = 1$. The situation changes dramatically when $|\epsilon_m| \gg \epsilon_d$ since now the local field are concentrated in the dielectric gaps between the conducting clusters achieving there the values E_m given by Eq. (34). The total current J_g of the electric displacement flowing in the dielectric gap between two resonate metal clusters of size l_r can be estimated as $J_g = aE_m \epsilon_e l_r^{(d-2)}$, where aE_m is the voltage drop across the gap, ϵ_e is effective dielectric constant of the composite. Because of the current continuity, the same current should flow in the adjacent metal clusters. In the metal cluster the current is concentrated in a percolating channel.[7,36] The electric field in the metal channel, which spans over the cluster, can be estimated as $E_{in} \sim J_g/(\epsilon_m a^{d-1})$. Then nth moment of the local electric field in a metal cluster of size l_r is equal to $\langle E_{in}^n \rangle = E_{in}^n \mathcal{L} a^{d-1}/l_r^d$, where $\mathcal{L}a^{d-1}$ is the volume of the conducting channel, $\mathcal{L} = a(\epsilon_m/\epsilon_e) l_r^{-d+2}$ is the effective length of the conducting channel. Now, we take into account that only the fraction $\kappa = \epsilon''_m/|\epsilon_m| \ll 1$ of metal clusters of size l_r are excited by the external electric field; then we obtain the following estimate for the moments $M_n^{(metal)} = \langle |E|^n \rangle_{metal} = \kappa \langle E_{in}^n \rangle$ of the local field averaged over the metal component only

$$M_n^{(metal)} \sim \left(\frac{|\epsilon_m|}{\epsilon''_m} \right)^{n-1} \left(\frac{|\epsilon_m|}{\epsilon_d} \right)^{\nu[n(d-1-t/\nu)+t/\nu+2-2d]/(t+s)}, \tag{65}$$

where we use expression (33) for the size l_r of the resonate clusters. For two-dimensional systems ($d=2$), where $t \cong s \cong \nu \cong 4/3$, we obtain from Eq. (65) $G_K^{metal} \sim M_4^{(metal)} \sim (|\epsilon_m|/\epsilon''_m)^3 (\epsilon_d/|\epsilon_m|)^{1/2}$. Computer simulation results for enhancement of the Kerr nonlinearity G_K^{metal} for silver semicontinuous film are shown in Fig. 6 as a function of the metal concentration p. From Figs. 5 and 6 we see $G_K^{metal} \ll G_K$ as expected. Near the percolation threshold we can compare G_K^{metal} and G_K quantitatively. Considering for simplicity $2d$ case, where $t \approx s \approx \nu$, and using Eqs. (64) and (65) we obtain

$$\frac{G_K}{G_K^{metal}} \sim \left(\frac{|\epsilon_m|}{\epsilon_d} \right)^2. \tag{66}$$

Thus, for $|\epsilon_m| \gg \epsilon_d$ the Kerr nonlinearity enhancement is much larger when the "seed" nonlinearity is located in the dielectric gaps where the local fields are much larger than in metal. It follows from Eq. (66) and also from Fig. 6 that the Kerr enhancement G_K^{metal} may become less than one. This means that local electric fields in the metal component can be smaller than the external field on average. For semicontinuous silver films on a glass substrate it happens for wavelength $\lambda > 10$ μm as one can see in Fig. 6.

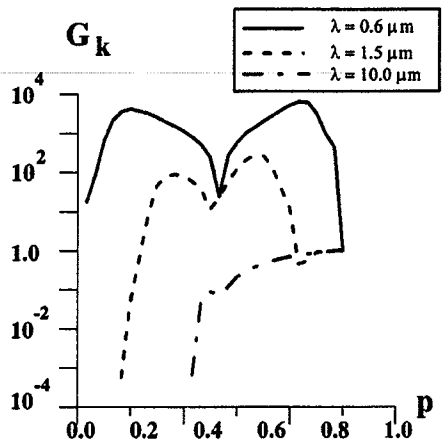

FIG. 6. Average enhancement of the Kerr optical nonlinearity $G_K^{metal} = M_{2,2}^{metal}$ in silver semicontinuous films as a function of the metal concentration p for three different wavelengths. The nonlinear Kerr permittivity $\epsilon^{(3)}$ is in the metal component only.

We also note here that enhancement for nearly degenerate four-wave mixing G_{FWM}, such as coherent anti-Stokes Raman scattering and optical phase conjugation process, is estimated as $G_{FWM} \sim |G_K|^2$ and can be very large.[10]

D. Discussion of models: Swiss-Cheese dielectric

So far, we restricted our consideration to the model containing only two types of elements, with metal dielectric function ϵ_m and dielectric constant ϵ_d and the volume concentrations p and $1-p$, respectively. The more realistic model of a metal-dielectric composite should take into account that metal elements can be different and characterized by some distribution $F(\epsilon_m)$. The same is true for dielectric elements whose properties in real percolation composites can vary over the system. We note that a narrow distribution of the parameters originating, for example, from different sizes of metal grains does not affect the critical exponents,[7,36] so that the above estimates for the field moments remain unchanged.

The situation changes, however, when a distribution of the internal parameters is broad, as in the Swiss-Cheese model[75] suggested for continuous media. In this model for the $3d$ case, while the critical index ν for the correlation length remains the same as in the lattice model, the transport exponents, such as t, can be different from their lattice values. For the $2d$ random checkerboard model[76] it was argued that the "dielectric" exponent s is different from the lattice value, while the percolation exponents remain the same.[77] It was shown in Ref. 78 that although the critical exponents for transport in continuous media may be different from the lattice values, they still satisfy the standard scaling relation of the statistical mechanics as do their lattice counterparts. So despite the fact that the values of the critical exponents in continuous media can be different we speculate that the corresponding functional dependencies may remain unchanged for a number of physical processes.

Very little is known about the effect of a broad parameter distribution on the local em fields. Consider, for example, the Swiss-Cheese model that can be mapped onto random R-C network with a broad distribution $f(R)$ of resistors R so that the average value $\langle R\rangle=\int f(R)dR=\infty$ diverges. The geometrical structure of the conducting "R" bonds does not depend on the distribution $f(R)$; therefore, the spatial inhomogeneity is still given by the percolation correlation length ξ for the resistor concentration p close to the percolation threshold. When all the conducting elements are the same, the conductance in the spatial scale ξ, according to the percolation theory, is determined by the "critical" chain of resistors.[36] The potential drop (and the local electric field) is approximately the same for the resistors in the critical chain and its resistance can be estimated as $\langle R\rangle\mathcal{L}$, where $\mathcal{L}$ is the length of the chain. On the other hand, for the Swiss-Cheese model the distribution $f(R)$ is so broad that the resistance of the critical chain is due to a single element with the largest resistance. Then the voltage drops mainly in this critical resistor, which determines the conductivity in the scale ξ. Note that the dependence of the critical exponent t on the resistance distribution $f(R)$ follows from this fact.[79–81]

The moments M_n of the local fields are power-law functions of the percolation correlation length $M_n\sim\xi^{q(n)}$, since ξ is a single spatial scale in the considered static case. When the local field concentrates in a single element (in the scale ξ) the critical exponent $q(n)$ acquires the form of a linear function of n, implying a constant gap between the exponents $q(n)$ for consecutive n. Therefore, the field distribution becomes compact and looses its multifractal nature for the Swiss-Cheese model.[36]

Contrary to these conclusions, in Ref. 82 it has been argued that for the Swiss-Cheese model in the "truly" continuous case the local-field distribution becomes wider. Analysis of a continuous metal film perforated by circular voids shows that the local field concentrates in narrow splits between the voids. This concentration of the field results in the power-law tails in the local field distribution (this analysis was also performed for the static field).

In the considered here case of optical properties, the continuous structure of a medium may affect the conductivity of metal clusters (e.g., the bottle-neck contacts between the metal grains) and result in renormalization of the exponent t in the formulas obtained above for the spatial moments of the local optical fields. This, however, does not affect the functional dependencies derived above.

The situation changes when a dielectric component is characterized by a broad distribution of parameters. Recall that the highest electric fields are concentrated in the dielectric gaps, rather than in metal clusters. In this case, not only the critical exponents may be renormalized but the corresponding functional dependencies may also be different.

We have shown in Sec. II B that the local electric field concentrates in a dielectric gap between resonating metal clusters of the size l^*. The voltage drop between the two resonating metal clusters can be estimated from Eq. (34) as $U_m=E_m a$, and the nth field moment averaged over the volume of the gap can be written as

$$\langle E^n\rangle_{gap}\sim\frac{U_m^n}{aS_{gap}}\int\frac{d\mathbf{q}}{x(\mathbf{q})^{n-1}}, \tag{67}$$

where $x(\mathbf{q})$ is the thickness of the gap (depending on the coordinate $\mathbf{q}$ along the gap) and the integration is over the gap area $S_{gap}\propto a^{d-1}n(l_r)$, where $n(l_r)$ is given by Eq. (40). Hereafter, we set, for simplicity, $E_0=1$.

We suppose now that the thickness x of a dielectric gap between two metal clusters is distributed as $f(x)$. Then Eq. (67) can be rewritten as

$$\langle E^n\rangle_{gap}\sim\frac{U_m^n}{a}\int_0^{x_{max}}\frac{f(x)}{x^{n-1}}dx. \tag{68}$$

Provided that the distribution $f(x)$ has a well-defined maximum near the granular size a, the average $\langle E^n\rangle_{gap}\sim E_m^n$, in accordance with previous considerations.

Now we consider the case when the gap distribution $f(x)$ does not vanish at $x\to 0$; for simplicity, we assume that the gap size x is distributed uniformly between 0 and a, i.e., $f(x)=a^{-1}$ for $0\leq x\leq a$. In this case the integral in Eq. (68) diverges at the lower limit and this equation cannot be used to estimate the field moments. In this case the integral in Eq. (67) is determined by the distance x_{min} for the closest approach of the clusters. Since the distances x are distributed uniformly in the segment $0\leq x\leq a$ the "effective" x_{min} can be estimated as $x_{min}\sim a/n(l_r)$, where the number of capacitance contacts, i.e., the "effective area" of the gap $n(l_r)$ is given by Eq. (40). By approximating the integral in Eq. (67) as $\sim a^{d-1}/x_{min}^{n-1}$ we obtain

$$\langle E^n\rangle_{gap}\sim\frac{U_m^n}{S_{gap}}\frac{a^{d-2}}{x_{min}^{n-1}}\sim E_m^n n(l_r)^{n-2}$$
$$\sim E_m^n(l_r/a)^{(d-2+s/\nu)(n-2)}. \tag{69}$$

By substituting this expression instead of E_m^n in Eq. (41), we obtain the new estimate for the field moments:

$$M_{n,m}\sim\rho(\xi_A/a)^{d-2(n+m)}\left(\frac{|\epsilon_m|}{\epsilon_d}\right)^{\{[s](n-2)+s\}/(s+t)}$$
$$\times\left(\frac{|\epsilon_m|}{\epsilon_m''}\right)^{n+m-1} \tag{70}$$

that holds for $n+m\geq 2$. Thus, we arrive at the conclusion that the field moments in the Swiss-dielectric model differ from those obtained previously for the discrete network by the factor $(|\epsilon_m|/\epsilon_d)^{(n-2)[\nu(d-2)+s]/s+t}$, which is much larger than one for $n+m>2$.

The spatial distribution of the local fields also changes significantly in the Swiss-dielectric model: instead of a chain of local maxima between resonating metal clusters we have a single peak with the amplitude $E_{max}\sim E_m(x_{min}/a)\sim E_m(|\epsilon_m|/\epsilon_d)^{[\nu(d-1)+s]/(s+t)}$, which is much larger than the previous estimate for E_m given by Eq. (34). We speculate that in this case, the maximum enhancement for the local-field is achieved since we have only one peak within the field correlation length ξ_e.

IV. CONCLUSIONS

In this paper we studied the local electric field distribution and enhancement of optical nonlinearities of random metal-

dielectric composites. We show that the surface plasmon (sp) modes are localized in metal-dielectric percolation composites, and the electric fields in such systems consist of sharp peaks resulting in very inhomogeneous spatial distributions of local fields. In peaks (''hot'' spots), the local fields exceed the applied field by several orders of magnitudes. These peaks are localized in nm-sized areas and can be associated with the eigenstates of the Kirchhoff's Hamiltonian. For any particular frequency in the visible and infrared spectral ranges we can find the eigenstates representing the sp resonance modes. The amount of metal grains supporting these resonance excitations is negligibly small in comparison with the total number of metal grains. Nevertheless, the resonant clusters cover the entire volume of the film because of their fractality. The incident light excites the resonance clusters and they interact with each other. As a result, the local field is concentrated in sharp peaks placed in some subset of the resonance clusters. The amplitudes of the peaks and the average distances between them increase with the wavelength.

The strongly fluctuating fields associated with the sharp peaks in various random parts of a film, result in giant enhancements of nonlinear optical processes since they are proportional to the enhanced local fields raised to a power greater than one. Because of such pattern for the local field distribution, the nonlinear signals are mostly generated from very small nm-sized areas.

We have obtained scaling formulas for enhancement of arbitrary nonlinear optical processes that in general depend not only on the field magnitudes but also on their phases. It was shown that the enhancement strongly depends, in terms of its magnitude and spectral dependence, on exact nature of the nonlinear process and can be different, even for processes with the same order of optical nonlinearity. Namely, it strongly depends on whether there is (at least one) act of photon subtraction in the multiphoton scattering leading to a generated wave. As a result, the enhancement for processes with photon subtraction, such as Raman and hyper-Raman scattering, Kerr-type nonlinear refraction and four-wave mixing, is significantly different from the enhancement for processes without photon subtraction, such as sum-frequency and high-harmonic generation.

Both the local and average enhancements for nonlinear optical processes strongly increase toward the long-wavelength part of the spectrum for two-dimensional system and decrease with increasing the wavelength for three-dimensional percolation systems. Note also that because the ''hot'' spots are localized in nm-sized areas and provide giant enhancement in their locations, a fascinating possibility of *nonlinear* spectroscopy of single molecules on a semicontinuous metal film becomes feasible. These nano-optical effects can be probed, for example, with near-field scanning optical microscopy providing sub-wavelength spatial resolution.

ACKNOWLEDGMENTS

This work was supported in part by NSF (Grant No. DMR-9810183), PRF, NATO, and RFFI (98-02-17628).

[1] *Statistical Models for the Fracture of Disordered Media*, edited by H.J. Herrmann and S. Roux, Elsevier Science Publisher B.V. (North-Holland, Amsterdam, 1990), and references therein.

[2] A. Aharony, Phys. Rev. Lett. **58**, 2726 (1987).

[3] D. Stroud and P.M. Hui, Phys. Rev. B **37**, 8719 (1988).

[4] V.M. Shalaev and M.I. Shtockman, Zh. Éksp. Teor. Fiz. **92**, 509 (1987) [Sov. Phys. JETP **65**, 287 (1987)]; A.V. Butenko, V.M. Shalaev, and M.I. Shtockman, *ibid.* **94**, 107 (1988) [**67**, 60 (1988)].

[5] A.P. Vinogradov, A.V. Goldenshtein, and A.K. Sarychev, Zh. Tekh. Fiz. **59**, 208 (1989) [Sov. Phys. Tech. Phys. **34**, 125 (1989)]; V.A. Garanov, A.A. Kalachev, A.M. Karimov, A.N. Lagarkov, S.M. Matytsin, A.B. Pakhomov, B.P. Peregood, A.K. Sarychev, A.P. Vinogradov, and A.M. Virnic, J. Phys. Condens. Matter **3**, 3367 (1991); V.A. Garanov, A.A. Kalachev, S.M. Matytsin, I.I. Oblakova, A.B. Pakhomov, and A.K. Sarychev, Zh. Tekh. Fiz. **62**, 44 (1992) [Sov. Phys. Techn. Phys. **37**, 506 (1992)].

[6] D.J. Bergman, Phys. Rev. B **39**, 4598 (1989).

[7] D.J. Bergman and D. Stroud, Solid State Phys. **46**, 14 (1992).

[8] P.M. Hui, in *Nonlinearity and Breakdown in Soft Condensed Matter*, edited by K.K. Bardhan, B.K. Chakrabarty, and A. Hansen, Lecture Notes in Physics (Springer Verlag, Berlin, 1996), Vol. 437.

[9] V.M. Shalaev, Phys. Rep. **272**, 61 (1996); *Nonlinear Optics of Random Media: Fractal Composites and Metal-Dielectric Films* (Springer-Verlag, Berlin, 1999).

[10] V.M. Shalaev and A.K. Sarychev, Phys. Rev. B **57**, 13 265 (1998).

[11] Hongru Ma, Rongfu Xiao, and Ping Sheng, J. Opt. Soc. Am. B **15**, 1022 (1998).

[12] D. Stroud, Superlattices Microstruct. **23**, 567 (1998).

[13] D. Bergman, O. Levy, and D. Stroud, Phys. Rev. B **49**, 129 (1994); O. Levy and D. Bergman, Physica A **207**, 157 (1994); O. Levy, D.J. Bergman, and D.G. Stroud, Phys. Rev. E **52**, 3184 (1995).

[14] R.W. Cohen, G.D. Cody, M.D. Coutts, and B. Abeles, Phys. Rev. B **8**, 3689 (1973).

[15] J.P. Clerc, G. Giraud, and J.M. Luck, Adv. Phys. **39**, 191 (1990).

[16] C. Flytzanis, Prog. Opt. **29**, 2539 (1992), and references therein.

[17] R.W. Boyd, *Nonlinear Optics* (Academic Press, New York, 1992); L.D. Landau, E.M. Lifshits, and L.P. Pitaevskii, *Electromagnetics of Continuous Media*, 2nd ed. (Pergamon, Oxford, 1984).

[18] Ping Shen, *Introduction to Wave Scattering, Localization, and Mesoscopic Phenomena* (Academic Press, San Diego, 1995).

[19] D.A.G. Bruggeman, Ann. Phys. (Leipzig) **24**, 636 (1935).

[20] X.C. Zeng, D.J. Bergman, P.M. Hui, and D. Stroud, Phys. Rev. B **38**, 10 970 (1988); X.C. Zeng, P.M. Hui, D.J. Bergman, and D. Stroud, Physica A **157**, 10 970 (1989).

[21] D.J. Bergman, in *Composite Media and Homogenization Theory*, edited by G. Dal Maso and G.F. Dell'Antinio (Brikhauser, Boston, 1991), p. 67.

[22] O. Levy and D.J. Bergman, J. Phys: Condens. Matter **5**, 7095 (1993).

[23] P.M. Hui and D. Stroud, Phys. Rev. B **49**, 11 729 (1994).

[24] H.C. Lee, K.P. Yuen, and K.W. Yu, Phys. Rev. B **51**, 9317 (1995).

[25] W.M.V. Wan, H.C. Lee, P.M. Hui, and K.W. Yu, Phys. Rev. B **54**, 3946 (1996).
[26] P.M. Hui, P. Cheung, and Y.R. Kwong, Physica A **241**, 301 (1997), and references therein.
[27] S. Blacher, F. Brouers, and A.K. Sarychev, in *Fractals in the Natural and Applied Sciences* (Chapman and Hall, London, 1995), Chap. 24.
[28] F. Brouers, A.K. Sarychev, S. Blacher, and O. Lothaire, Physica A **241**, 146 (1997).
[29] F. Brouers, S. Blacher, and A.K. Sarychev, Phys. Rev. B **58**, 15 897 (1998).
[30] F. Brouers, S. Blacher, A.N. Lagarkov, A.K. Sarychev, P. Gadenne, and V.M. Shalaev, Phys. Rev. B **55**, 13 234 (1997).
[31] P. Gadenne, F. Brouers, V.M. Shalaev, and A.K. Sarychev, J. Opt. Soc. Am. B **15**, 68 (1998).
[32] D.P. Tsai, J. Kovacs, Z.H. Wang, M. Moskovits, V.M. Shalaev, J.S. Suh, and R.D. Botet, Phys. Rev. Lett. **72**, 4149 (1994); V.P. Safonov, V.M. Shalaev, V.A. Markel, Y.E. Danilova, N.N. Lepeshkin, W. Kim, S.G. Rautian, and R.L. Armstrong, *ibid.* **80**, 1102 (1998); V. A. Markel, V. M. Shalaev, P. Zhang, W. Huynh, L. Tay, T.L. Haslett, and M. Moskovits, Phys. Rev. B **59**, 10 903 (1999).
[33] S.I. Bozhevolnyi, I.I. Smolyaninov, and A.V. Zayats, Phys. Rev. B **51**, 17 916 (1995); S.I. Bozhevolnyi, V.A. Markel, V. Coello, W. Kim, and V.M. Shalaev, Phys. Rev. B **58**, 11 441 (1998).
[34] A.N. Lagarkov, K.N. Rozanov, A.K. Sarychev, and A.N. Simonov, Physica A **241**, 199 (1997).
[35] S. Grésillon, L. Aigouy, A.C. Boccara, J.C. Rivoal, X. Quelin, C. Desmarest, P. Gadenne, V.A. Shubin, A.K. Sarychev, and V.M. Shalaev, Phys. Rev. Lett. **82**, 4520 (1999).
[36] D. Stauffer and A. Aharony, *An Introduction to Percolation Theory*, 2nd ed. (Taylor and Francis, London, 1994).
[37] H.E. Stanley, *Introduction to Phase Transition and Critical Phenomena* (Oxford University Press, Oxford, 1981); I.L. Fabelinskii, *Molecular Scattering of Light* (Plenum, NY, 1968).
[38] P.M. Chaikin and T.C. Lubensky, *Principles of Condensed Matter Physics* (Cambridge University Press, Cambridge, 1995).
[39] A. Aharony, R. Blumenfeld, and A.B. Harris, Phys. Rev. B **47**, 5756 (1993).
[40] D. Stroud and X. Zhang, Physica A **207**, 55 (1994); X. Zhang and D. Stroud, Phys. Rev. B **49**, 944 (1994).
[41] B. Kramer and A. MacKinnon, Rep. Prog. Phys. **56**, 1469 (1993).
[42] D. Belitz and T.R. Kirkpatrick, Rev. Mod. Phys. **66**, 261 (1994).
[43] M.V. Sadovskii, Phys. Rep. **282**, 225 (1997).
[44] K.B. Efetov, *Supersymmetry in Disorder and Chaos* (Cambridge University Press, UK, 1997).
[45] J.A. Verges, Phys. Rev. B **57**, 870 (1998).
[46] A. Elimes, R.A. Romer, and M. Schreiber, Eur. Phys. J. B **1**, 29 (1998).
[47] T. Kawarabayashi, B. Kramer, and T. Ohtsuki, Phys. Rev. B **57**, 11 842 (1998).
[48] V.I. Fal'ko and K.B. Efetov, Phys. Rev. B **52**, 17 413 (1995).
[49] K. Muller *et al.*, Phys. Rev. Lett. **78**, 215 (1997).
[50] M.V. Berry, J. Phys. A **10**, 2083 (1977).
[51] A.V. Andreev, O. Agam, B.D. Simons, and B.L. Altschuler, Phys. Rev. Lett. **76**, 3947 (1996).
[52] M.I. Stockman, L.N. Pandey, L.S. Muratov, and T.F. George, Phys. Rev. Lett. **72**, 2486 (1994); M.I. Stockman, L.N. Pandey, L.S. Muratov, and T.F. George, Phys. Rev. B **51**, 185 (1995); M.I. Stockman, L.N. Pandey, and T.F. George, *ibid.* **53**, 2183 (1996).
[53] M. Kaveh and N.F. Mott, J. Phys. A **14**, 259 (1981).
[54] I.E. Smolyarenko and B.L. Altshuler, Phys. Rev. B **55**, 10 451 (1997).
[55] V.M. Shalaev, E.Y. Poliakov, and V.A. Markel, Phys. Rev. B **53**, 2437 (1996); V.A. Markel, V.M. Shalaev, E.B. Stechel, W. Kim, and R.L. Armstrong, *ibid.* **53**, 2425 (1996).
[56] M.I. Stockman, Phys. Rev. E **56**, 6494 (1997); Phys. Rev. Lett. **79**, 4562 (1997).
[57] *Handbook of Optical Constants of Solids*, edited by E.D. Palik (Academic Press, NY, 1985); P.B. Johnson and R.W. Christy, Phys. Rev. B **6**, 4370 (1972).
[58] A.N. Lagarkov, A.K. Sarychev, Y.R. Smychkovich, and A.P. Vinogradov, J. Electromagn. Waves Appl. **6**, 1159 (1992).
[59] P.J. Reynolds, W. Klein, and H.E. Stanley, J. Phys. C **10**, L167 (1977); A.K. Sarychev, Zh. Éksp. Teor. Fiz. **72**, 1001 (1977) [Sov. Phys. JETP **45**, 524 (1977)].
[60] A. Liebsch and W. L. Schaich, Phys. Rev. B **40**, 5401 (1989).
[61] R. Murphy, M. Yeganeh, K.J. Song, and E.W. Plummer, Phys. Rev. Lett. **63**, 318 (1989).
[62] G.A. Reider and T.F. Heinz, in *Photonic Probes of Surfaces: Electromagnetic Waves*, edited by P. Halevi (Elsevier, New York, 1995).
[63] T.Y.F. Tsang, Phys. Rev. A **52**, 4116 (1995).
[64] R.A. Watts, T.W. Preist, and J.R. Sambles, Phys. Rev. Lett. **79**, 3978 (1997).
[65] A.R. McGurn, A.A. Maradudin, and V. Celli, Phys. Rev. B **31**, 4866 (1985); A. R. McGurn, Surf. Sci. Rep. **10**, 359 (1990).
[66] J.A. Sanchez-Gil, A.A. Maradudin, J.Q. Lu, V.D. Freilikher, M. Pustilnik, and I. Yurkevich, Phys. Rev. B **50**, 15 353 (1994).
[67] L. Kuang and H.J. Simon, Phys. Lett. A **197**, 257 (1995).
[68] T.Y.F. Tsang, Opt. Lett. **21**, 245 (1996).
[69] B. Hecht, H. Bielefeldt, L. Novotny, Y. Inouye, and D.W. Pohl, Phys. Rev. Lett. **77**, 1889 (1996).
[70] A.K. Sarychev, V.A. Shubin, and V.M. Shalaev, Phys. Rev. E **59**, 7239 (1999).
[71] O.A. Aktsipetrov, O. Keller, K. Pedersen, A.A. Nikulin, N.N. Novikova, and A.A. Fedyanin, Phys. Lett. A **179**, 149 (1993).
[72] M. Moskovits, Rev. Mod. Phys. **57**, 783 (1985).
[73] K. Kneipp, Y. Wang, H. Kneipp, Lt. Perelman, I. Itzkan, R. Dasari, and Ms. Feld, Phys. Rev. Lett. **78**, 1667 (1997).
[74] S. Nie and S.R. Emory, Science **275**, 1102 (1997).
[75] B.I. Halperin, S. Feng, and P.N. Sen, Phys. Rev. Lett. **54**, 2391 (1985); S. Feng, B.I. Halperin, and P.N. Sen, Phys. Rev. B **35**, 197 (1987).
[76] P. Sheng and R.V. Kohn, Phys. Rev. B **26**, 1331 (1982).
[77] L. Berlyand and K. Golden, Phys. Rev. B **50**, 2114 (1994).
[78] K. Golden, Phys. Rev. Lett. **78**, 3935 (1997).
[79] P.M. Cogut and J.P. Straley, J. Phys. C **12**, 2151 (1979).
[80] A. Ben-Mizrahi and D. Bergman, J. Phys. C **14**, 909 (1981).
[81] J.P. Straley, J. Phys. C **15**, 2333 (1982).
[82] E.M. Baskin and M.V. Entin, Phys. Low-Dimens. Semicond. Struct. **1/2**, 17 (1997).